Study of new optical blinking phenomena on InGaN/GaN single quantum well

2020

Master's thesis

Yokohama City University

Graduate School of Nanobioscience

Department of Materials System Science

Yusuke Fujii

CONTENTS

Study of new optical blinking phenomena on InGaN/GaN single quantum well

Author: Yusuke Fujii

Supervisor: Ruggero Micheletto

Subadvisors: Masanori Tachikawa

Subadvisors: Hirokazu Tanimoto

Study of new optical blinking phenomena on InGaN/GaN single quantum well

Department of Materials System Science　Yusuke Fujii

Supervisor　Ruggero Micheletto

[KeyWords]

- Blinking Phenomena: A phenomena in which a luminescent region of a few microns in size blinks unsteadily when a sample is excited. In 2006, The blinking phenomena in InGaN/GaN Single Quantum Well was first discovered by R. Micheletto *et al*. [1].
- InGaN/GaN Single Quantum Well (InGaN/GaN SQW): A structure in which an InGaN layer with a smaller band gap due to the addition of indium is sandwiched between two GaN layers with a larger band gap.
- Quantum Confined Stark Effect (QCSE): The generation of a piezoelectric field inside the sample, which causes the separation of the electron and hole wavefunctions and a decrease in the recombination rate.[2] It is thought that blinking is caused by the repeated increase and decrease in the overlap of the wave functions.

[Introduction]

Indium gallium nitride (InGaN) is now used as a material for blue light emitting diodes, and by changing the composition ratio of indium, it has become possible to cover not only blue but also wavelengths in most visible light regions. It is a device that is attracting a great deal of attention because it emits light with high brightness and long life. However, many things have not been clarified about this physical property. Among them, this study deals with the blinking phenomena.[1] Irradiation of InGaN/GaN Single Quantum Well by ultra violet with emission wavelength of 365nm as an excitation light results in the formation of localized domains where the optical emission is unstable. It is considered that lattice mismatch and high dislocation due to the use of sapphire substrate causes blinking phenomena, but it is not clear why blinking occurs. In this study, I attempted to clarify the physics mechanism of the blinking phenomena by using InGaN/GaN SQW.

[Method]

I used InGaN/GaN SQW with emission wavelengths of 460nm and 510nm provided by Prof. Yoichi Kawakami of Kyoto University as the measurement samples. This sample was grown by the metal-organic vapor deposition method, and has a double heterostructure consisting of a 4μm GaN layer, a 3nm InGaN layer, and a 5nm GaN layer in sequence on a sapphire substrate. As a measurement system, I used a selective excitation fluorescence microscope. The blinking was photographed by a 3CCD camera attached to the top of the microscope, and the data was sent to a computer for analysis. In this study, I explored the temperature dependence, the change in blinking due to the adhesion of liquid, and the characteristics of the blinking points by conducting statistical analysis.

[Results and Discussion]

(1) Temperature dependence:

The temperature dependence of the blinking phenomena is tested using a standard deviation map. InGaN/GaN SQW was placed on the heater, the temperature was changed from 300K to 373K, and the change in blinking was investigated. As a result, the emission wavelengths of both 460 nm and 510 nm blinked most strongly in the relatively low temperature range, but the blinking tended to become weaker at higher temperatures. At 373K, the 460nm sample was barely blinking, but the 510nm sample was still blinking. It is thought that one of the factors that alleviate the intensity of blinking due to temperature rise is that thermal expansion increases the defect density, making it easier for carriers to be trapped, and as a result, non-radiative recombination has done that does not emit light. However, since various physical quantities such as electron mobility change with temperature, it was not possible to identify a clear cause in this survey.

(2) Change in blinking phenomena due to liquid adhesion:

I have found that blinking is induced by the adhesion of liquid. In this study, water and ethanol were utilized and measured while adhering to the sample. When water was attached to the sample, the number of blinking points increased and the blinking was weak, but when ethanol was attached to the sample, the blinking tended to be incredibly intense. This was commonly observed for InGaN/GaN SQW with emission wavelengths of 460nm and 510nm.

If the blinking phenomena is caused by QCSE, it is considered that the liquid would have the effect of rapidly intensifying and weakening the magnitude of the piezoelectric field. The optical intensity at the blinking points also increased, suggesting that the liquid may be creating a state that promotes electronic excitation.

(3) Correlation among blinking points

By enlarging the blinking points displayed on the standard deviation map, I found several blinking points where two areas are blinking significantly. When I calculated the correlation of the other to one of these locations, it became clear that the regions blinked with negative correlation to each other. By expanding this to the entire area, the correlation was also shown with other blinking points in the surrounding area, and it became clear that the other blinking points are composed of two regions with negative correlation. The correlation here means the correlation of optical intensity in time series. The intensity of each blinking point was also

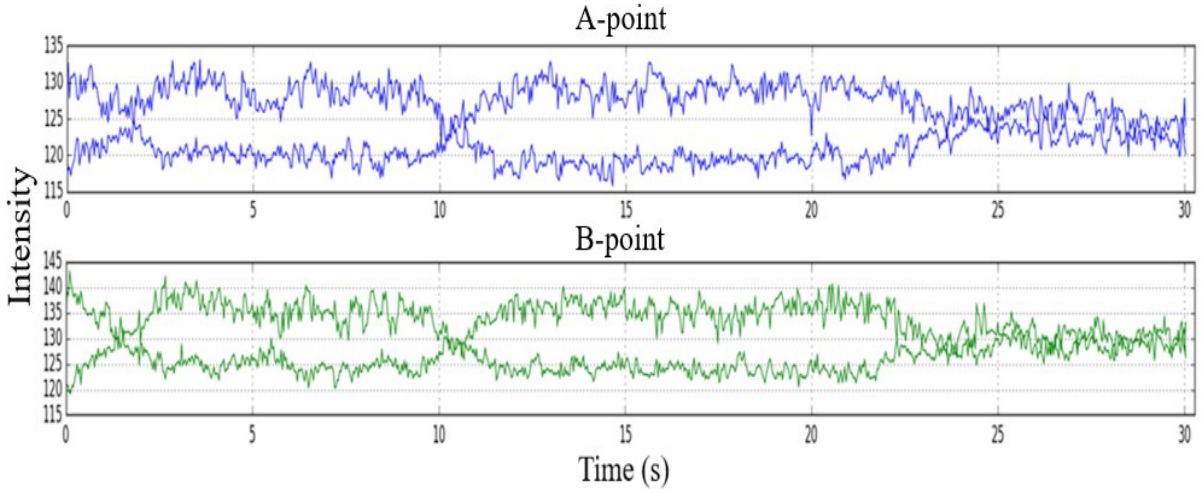

plotted in time series by region. It was found that the intensity of the blinking points seemed to be synchronized even though they are spatially different. If the blinking phenomena is caused by QCSE, it is considered that the magnitude of application of the piezo electric field is also synchronized.

Fig1. Time series data of optical intensities in two regions consisting of negatively correlated. A-point and B-point are spatially distinct blinking points.

[Bibliography]

[1] R.Micheletto *et al.* Appl. Phys. Lett. 88,061118 (2006)

[2] J.W.Robinson *et al.* Appl. Phys. Lett. 86,213103 (2005)

【日本語概要】

発光デバイスの1つでもあるInGaN/GaN単一量子井戸型構造に対し、光励起を行うと不安定な点滅を繰り返す輝点が無数に発生する。しかしながら、この点滅現象は未だ原因不明であり、メカニズムの解明が求められている。そこで、本研究では点滅現象の物理学的なメカニズムを解明することを目的とした。温度依存性、液体の付着による点滅現象の変化を追究したところ、これらの要素が点滅へ強い影響を及ぼしている事が分かった。また統計的な分析を進めることで、点滅点同士の相関性も明らかにした。

1 Introduction

1.1 History of InGaN and its application to the present

In modern society, Indium Gallium Nitride (InGaN) is used as a material for blue light-emitting diodes, which are used in home appliances, traffic lights, and Christmas lights. LEDs have the advantages of long life, high efficiency, and even lower power consumption, and are a good alternative to the traditional incandescent bulbs. There is a trend to move to LED bulbs and the number of users is expected to increase. This feature is expected to be used in the next generation of medical devices and new displays.

In 1989, blue light-emitting diodes had not yet been developed while yellow, red and yellow-green diodes were being developed. However, the creation of blue light-emitting diodes was made possible by Isamu Akasaki and Hiroshi Amano, who won the Nobel Prize in Physics in 2014; the pair succeeded in creating the world's first blue light-emitting diode, but the light intensity was 10 mcd and the emission wavelength was very dark, close to violet, at 470nm. Four years later, however, in 1993, Shuji Nakamura and his colleagues at Tokushima's Nichia Corporation succeeded in developing a blue light-emitting diode with high luminance and long life, although this was thought to be impossible. They were also able to create white LEDs from the three primary colors of light. This breakthrough was made possible by InGaN. Previously, silicon carbide was used as a material for semiconductor devices, but by switching to InGaN, which has a higher electron mobility than silicon, it can now be used as a material for high-frequency devices.[1]

As the implementation phase of what was adopted in the Paris Agreement began in 2020, we must focus our efforts on combating global warming. It is about keeping the average global temperature rise well below 2 degrees Celsius and limiting it to 1.5 degrees Celsius compared to the pre-industrial period. What we can do to achieve this goal is to reduce carbon dioxide emissions, and the practical application of LEDs will reduce electricity consumption and carbon dioxide emissions from thermal power plants. If all the incandescent light bulbs in Japan could be converted to LEDs, the energy equivalent of 4.5 power plants could be saved. From this point of view, the development of light-emitting devices based on InGaN is attracting attention for its environmental benefits.

1.2 Physical properties of InGaN material

1.2.1 $In_xGa_{(1-x)}N$

$In_xGa_{(1-x)}N$ is a mixed crystal of Indium Nitride (InN) and Gallium Nitride (GaN), and its bandgap value can be adjusted from infrared to ultraviolet light by changing the Indium composition ratio. This means that the material covers the wavelengths of visible light, making it possible to emit light in colors we can see. Figure1.1 shows the relationship between the lattice parameter and bandgap of group Ⅲ nitride semiconductors and other semiconductor materials.[2] It can be seen that the band gap of InN and GaN traverse visible light. The materials GaN and InN have many thermodynamically stable hexagonal wurtzite type structures as shown in Figure1.2 [3]

1.2.2 Vegard's law

The $In_xGa_{(1-x)}N$ band gap becomes smaller as the Indium composition ratio increases, and the emission wavelength shifts to longer wavelengths. This relationship follows the Vegard's law. The Vegard's law is a relationship between the composition ratio and the band gap, as shown in the following equation (1).

$$E_{g.InGaN}(x) = x\,E_{g.InN} + (1-x)E_{g,GaN} - bx(1-x) \qquad (1)$$

$E_{g.InN}$ represents the band gap of InN (0.65eV), and similarly, $E_{g,GaN}$ represents the bandgap of GaN (3.4eV). x indicates the amount of Indium. b is called the Bowing parameter. Figure1.3 is a plot of the relationship between the composition of Indium and the band gap when the bowing parameter is set to 1. According to this figure, As the indium composition increases, the band gap decreases exponentially and the emission wavelength shifts to higher wavelengths.

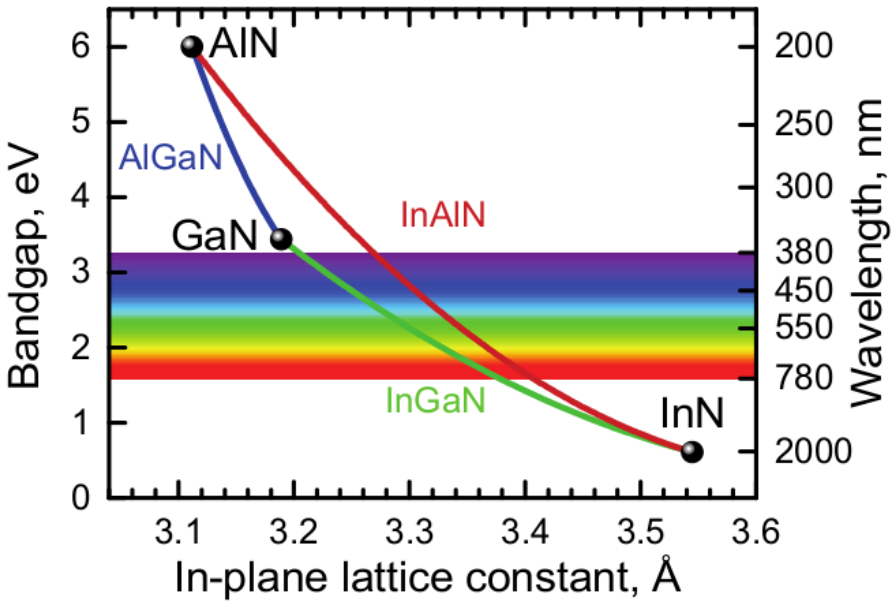

Figure1.1 Relationship between lattice parameter and band gap of wurtzite structure [2]

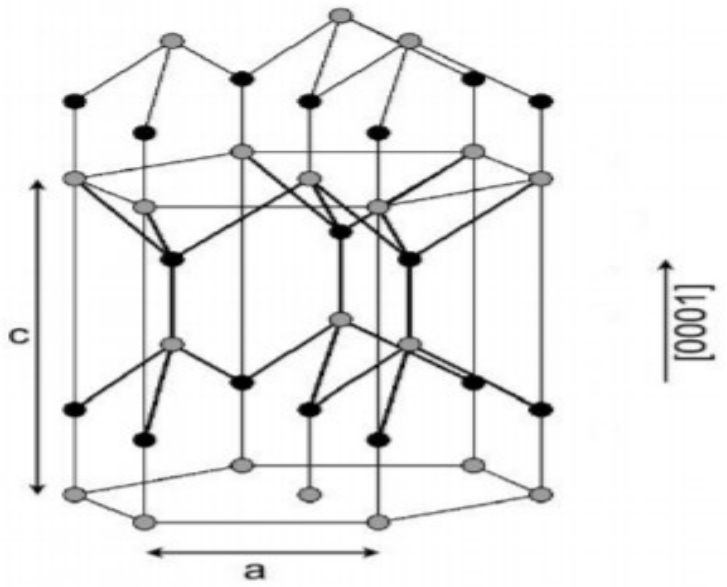

Figure1.2 GaN crystal with a hexagonal wurtzite structure; InN crystal has a similar structure. black is nitrogen and gray is gallium or indium. [3]

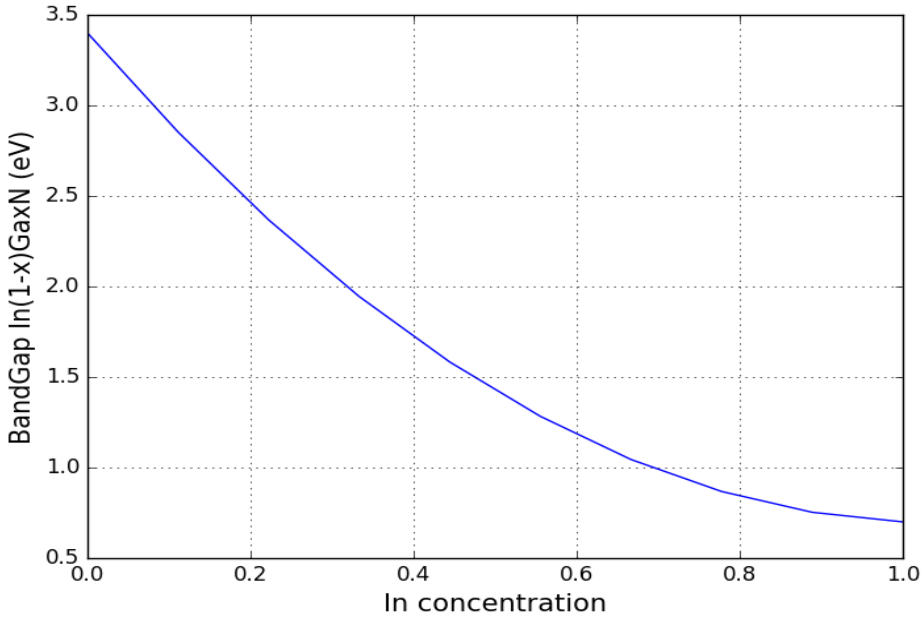

Figure1.3 The relationship between the concentration of Indium and the band gap according to the Vegard's law, with Bowing set to 1. The band gap decreases exponentially as the concentration of Indium increases

1.2.3 Structural defects and their effects

There is no substrate suitable for the epitaxial growth of GaN material with a perfect lattice constant. For this reason, sapphire is often used as substrate because their lattice constants are close to those of other substrates, they are relatively inexpensive, and they can withstand high temperatures. However, even if sapphires are used, the thermal expansion coefficients and lattice constants are very different, which leads to large structural defects and threading dislocation.[4] Table 1.1 lists the lattice parameters, thermal conductivity, and coefficient of thermal expansion for various materials used as a substrate.[5] These defects have a negative impact on the entire devise. The formation of the threading dislocation traps electrons in deep levels and converts the light energy caused by the recombination of electrons and holes into thermal energy. The phenomena is called nonradiative recombination. How an LED using InGaN as the luminescent layer could shine so brightly despite the formation of many defects that cause nonradiative recombination had been a mystery. However, Y. Narukawa *et al*. concluded that fluctuations in the composition of Indium can cause excitons to move to sites where indium with lower potential is localized, resulting in luminescent recombination. [6,7] In fact, by using SNOM, they show that InGaN emits blue light where the potential is concave. [8]

The mechanism of high brightness luminescence in spite of many structural defects is being elucidated. However, there are several phenomena in InGaN that have not yet been resolved, which are thought to be caused by structural defects. One of them is the key to this thesis: Blinking Phenomena. [9] I discuss the phenomena in detail in Chapter 2. The Blinking phenomena is considered to be caused by a structural defect, but the physical mechanism is not yet understood.

Table1.1 Substrates used in III-V nitride semiconductors and their physical properties. [5]

Substrate material	Lattice Parameters	Thermal Conductivity	Coefficients of thermal expansion
GaN	a=3.189Å c=5.185Å	1.3W/cm K	5.59×10^{-6}/K 3.17×10^{-6}/K
AlN	a=3.112Å c=4.982Å	2.0W/cm K	4.2×10^{-6}/K 5.3×10^{-6}/K
6H SiC	a=3.08Å c=15.12Å	4.9W/cm K	4.2×10^{-6}/K 4.68×10^{-6}/K
Sapphire	a=4.758Å c=12.99Å	0.5W/cm K	7.5×10^{-6}/K 8.5×10^{-6}/K

1.3 Research Purpose

The purpose of this study is to elucidate the unexplained optical properties of InGaN materials for blue LED light emitting devices. In particular, I focus on the "blinking phenomena" discovered by R. Micheletto *et al*. in 2006.[9] As mentioned above, there is no physical model that can explain blinking phenomena. In an ideal structure, the blinking phenomena would not occur. If the physical mechanism of the blinking phenomena is clarified, it leads to the development of a very innovative new device. A detailed explanation of the blinking phenomena, possible theoretical models, and examples of previous research discuss in Chapter 2. In this study, I used two types of InGaN/GaN single quantum well (SQW) structures with emission center wavelengths of 460nm and 510nm. A detailed description of the samples is given in Chapter 3.

In this study, I investigated the characteristics of blinking by analyzing the temperature dependence of the blinking phenomena, the change caused by the adhesion of liquid, and statistical analysis, and from these results, I attempted to clarify the physical mechanism of the blinking occurrence.

1.4 Structure of this thesis

Chapter 1 summarizes the history of the development of InGaN nitride semiconductors and their universal physical properties.

Chapter 2 summarizes the specific explanation of the blinking phenomena, the physical model that is considered to be the cause of the blinking phenomena, and examples of previous research.

Chapter 3 summarizes the experimental samples, the selective excitation fluorescence microscope used in this study, and the details of the processing of the obtained video data.

Chapter 4, the temperature dependence of the blinking phenomenon in the range of 300K to 373K is investigated using InGaN/GaN SQW with emission center wavelengths of 460nm and 510nm.

Chapter 5, I observed the blinking behavior by photoexcitation with a liquid attached. The liquids which I used were water and ethanol, and a comparison was made with the state without any liquid attached. As in Chapter 4, two types of samples with emission wavelengths of 460nm and 510nm were utilized.

Chapter 6, I discuss what was revealed by proceeding with the statistical analysis, such as standard deviation map and correlation map.

Chapter 7, I summarize our collaborative work with Dr. Giovanni Alfieri at Hitachi Power grip in Switzerland. It has been suggested that chlorine can be contaminated in reactive ion

etching, one of the production processes of gallium nitride (GaN), and the physical properties of GaN when contaminated with chlorine have not been clarified. Therefore, we investigated the electronic properties of GaN with impurity chlorine by performing the density functional theory using SIESTA, one of the first-principles calculation software. Since this is not my main research, I only briefly describe it.

The following chapter 8 consists of references, chapter 9 consists of acknowledgments, chapter 10 contains research achievements, and the last chapter 11 contains the abstract of this thesis in Japanese.

2 Blinking Phenomena on InGaN/GaN SQW

2.1 Blinking Phenomena

Irradiating the surface of an InGaN/GaN SQW used in a light emitting device with narrow-band ultraviolet light produces a myriad of bright spots that repeat unstable blinking. This is the blinking phenomenon, and it is roughly a few microns in size. In 2006, R. Micheletto first observed the blinking phenomena in InGaN/GaN SQW growing in the [0001] direction on a sapphire substrate.[9] The phenomena occurs most often when only the peak of 365nm is taken out from the wavelengths irradiated from the mercury lamp and irradiated on the sample as excitation light. The observed blinking phenomena is shown in Figure2.1 and this data is for InGaN/GaN SQW with an emission wavelength of 510nm. In addition to this, samples with emission wavelengths of 460nm and 540nm were used and the blinking of the three samples were observed, there is a data that the longer the emission wavelength is, the more likely the blinking occurs.[3] As mentioned above, the ideal InGaN/GaN SQW does not cause blinking phenomena. Many physical models of the blinking phenomena have been proposed, but there is no physical model that we can use. In addition to InGaN, blinking phenomena have also been observed in quantum dots such as InP[10] and GaAs [11]. The next section describes some of the proposed models.

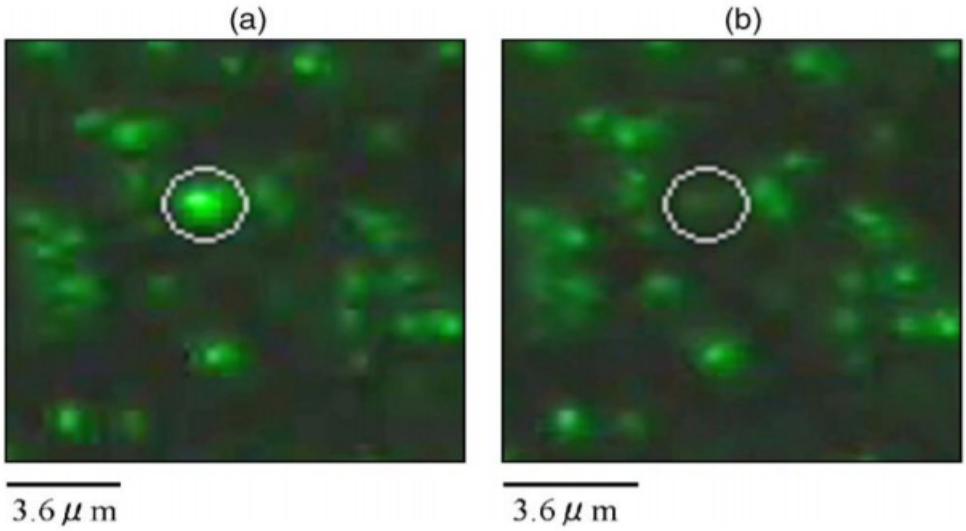

Figure2.1 A blinking point is circled. (a) is on-time and (b) is off-time. Sample is 510nm InGaN/GaN SQW [9]

2.2 For the proposed model of the blinking phenomena

In this section, I describe the model of the blinking phenomena that has been proposed.

1. Quantum Confined Stark Effect (QCSE)

The generation of a piezoelectric field inside the sample, which causes the separation of the electron and hole wavefunctions and a decrease in the recombination rate, is called Quantum Confined Stark Effect (QCSE).[12] In nitride semiconductors, two types of electric fields are generated: spontaneous electric fields and piezoelectric fields. The spontaneous electric field is generated due to the lack of symmetry of the crystal in the C-axis direction. The piezoelectric field is caused by a lattice constant mismatch with the substrate. InGaN/GaN SQW based on sapphire substrates are considered to have a large lattice mismatch, which may lead to a large piezoelectric field. Repeatedly overlapping and pulling apart of the wavefunctions could be the result of blinking mechanism. Figure2.2 shows a simple

schematic diagram of QCSE. This figure is taken from a master's thesis by K.Oikawa who graduated from our laboratory and is partially modified.[14]

Due to the distortion of the bandgap, the effective bandgap becomes smaller in the order of (a), (b), (c). Therefore, it is theoretically considered that the emission wavelength shifts to the longer wavelength side as the band gap is distorted. Experimental research is also being conducted to measure the spectra of (a) when the blinking light intensity is high (on-state) and (c) when the blinking light intensity is low (off-state). According to the Figure2.6 which is introduced in the next section, the blinking emission wavelengths are mostly distributed in the low wavelengths in the on-state, but the emission wavelengths are mostly distributed in the high wavelengths in the off-state. Therefore, from the perspective of both theory and experimental results, the hypothesis that the blinking phenomenon is caused by QCSE is very credible.

Since the piezoelectric field is detrimental to the device, some research has been done to reduce the piezoelectric field. For example, it has been reported that QCSE is suppressed for samples with quantum well type structures created on substrates with different surface orientations.[13]

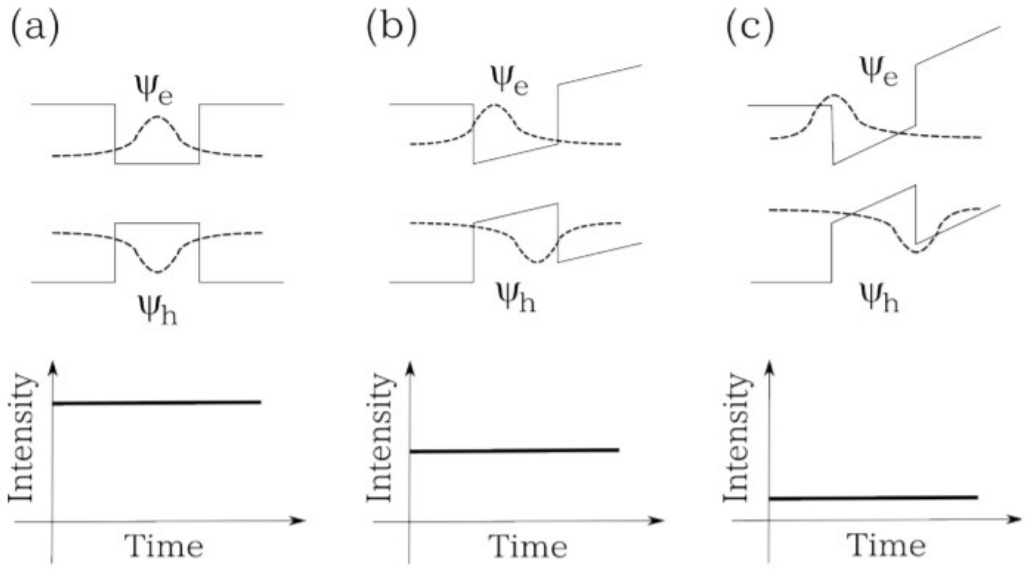

Figure2.2 A simple model of the causal relationship between QCSE and blinking phenomena in InGaN/GaN SQW. As the piezoelectric field increases, the overlap of the wave function decreases and the recombination rate of electrons and holes decreases. As a result, the emission intensity also decreases. The blinking phenomena can be considered as a repetition of (a), (b) and (c).[14]

2. Quantum Jump Model

A quantum jump model has been proposed by Cook and Kimble.[15] The ground state is considered to be 0 and the excited state is set to 1. In addition to these two, there is also a metastable state 2. Radiative recombination occurs as the carriers move back and forth between the 0⇆1 states. However, there are occasional carrier jumps to state 2 at random. Carriers transitioning to state 2 are non-radiative recombination and therefore do not encourage emission. This quantum jump model can be used as a theoretical model of the blinking phenomena by applying it to the rate equation.

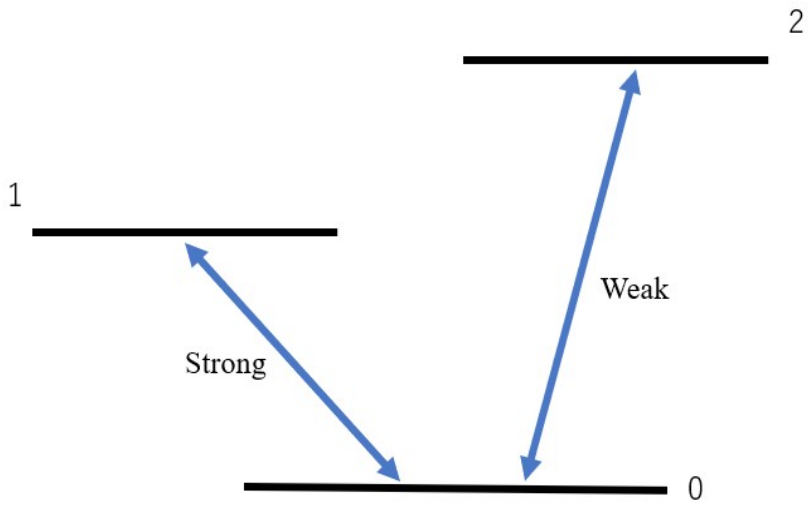

Figure2.3 Simple Energy-level scheme [15]

3. Auger Ionization

The on/off state of emission in quantum dots is consistent with the Auger ionization mechanism.[16] Quantum dots usually have a carrier or a single electron-hole pair. However, if there are two electron-hole pairs, when one electron-hole pair recombines, the energy released from the recombination is given to the other electron, which transitions to the trap level. The electrons in the trap level do not contribute to the luminescence because of the non-radiative recombination. Therefore, the radiative recombination rate is reduced, which has a negative effect on the luminescence.

2.3 Previous studies on the blinking phenomena in InGaN/GaN SQW

The blinking phenomena of InGaN/GaN SQW was discovered by R. Micheletto *et al*. in 2006. [9] They used a sample grown in the [0001] direction on a sapphire substrate with an emission wavelength of 510nm. This was made under the same conditions by the same preparers as the sample used in my research. The details of the samples describe in Chapter 3. According to their research, in Figure2.4, the blinking phenomena does not occur at 405nm, where only the quantum well layer is excited, but it occurs at 365nm, where the quantum well and GaN layer are excited, so it was suggested that the carriers flowing from the GaN layer to

the InGaN quantum well layer are not spatially uniform. Blinking can be divided into two types: those that move back and forth between the two intensities and those that behave continuously and chaotically. Details are in Figure2.5 They measured the wavelengths of the blinking when the light is on and off. As shown in Figure2.6, the spectra shifted to the low energy side when the light is on and to the high energy side when the light is off.

The temperature of the blinking phenomena has also been reported. As shown in Figure2.7, the temperature dependence of the blinking phenomena is measured every 10K in the range of 200 K to 290 K, it is the result of a 70-second exposure to excitation light with emission peak 365nm. The graph shows that the intensity and amplitude of the blinking increased as the temperature increased. Figure2.8 shows a histogram of the luminescence intensity at each temperature. The luminescence intensity shifts to higher intensity as the temperature is increased, and a wide range of values are taken.

T.Toshiaki *et al*. who graduated from our laboratory also reported on the temperature and pressure dependence of the total emission of InGaN/GaN SQW.[17] [18] The sample is a similar one grown in the [0001] direction on a sapphire substrate, with an emission wavelength of 540nm.

First of all, I discuss the temperature dependence of the experiment: Tsutsumi used a temperature control device (Cryogenic Control System's Model 32) to observe the luminescence change of InGaN/GaN SQW between 290 K and 320 K in atmospheric air. A sample is placed on a heater connected to the temperature control device and the temperature of the heater is simply changed. He measured the temperature dependence at 365nm and 405nm excitation light, respectively, and I will discuss the 365nm results in this paper. Figure2.9 shows the changes in temperature and emission intensity while the sample was

excited with 365nm. Figure2.9 shows the changes in temperature and emission intensity while exciting the sample with 365nm excitation light for 2000 seconds. The results show that as the temperature increases, the total emission increases, and conversely, as the temperature decreases, the total emission tends to decrease. As for the number of blinking points, he concludes qualitatively that the number does not change. So, Quantitative data have not been obtained on how the blinking flashes due to temperature changes.

Next, I report on the pressure dependence. The sample was placed in a vacuum chamber (RC102-CFM, CIA, Inc.) and the luminescence change was observed as the pressure was reduced from 1000 mmbr to 10^{-5} mmbr. As shown in Figure2.10, the overall luminescence intensity tended to gradually increase as the pressure is reduced. Conversely, when the pressure is increased rapidly, the total emission decrease. Although the result is qualitative, there is a tendency for the blinking points to decrease with decreasing pressure. Therefore, it can be suggested that the blinking may be induced by surface deposits.

Based on these results, they modeled the changes in the amount of adsorption and the overall luminescence intensity using an equation, assuming that the luminescence intensity decreases as the amount of physisorption increases and increases as the amount of physisorption decreases. Set the luminescence intensity be I(t). Assuming that this is proportional to the amount of adsorbed material on the surface, n(t), it can be expressed as follows.

$$I(t) = -\beta \times n(t) + I_{max} \qquad (1)$$

Where β is the loss of luminosity they set and I_{max} represents the maximum luminescence intensity. Furthermore, the time evolution of $n(t)$ is expressed by the following equation.

$$\frac{dn(t)}{dt} = -n(t)\gamma_{des}(t) + \left(n_{max} - n(t)\right)\gamma_{¿I(t)¿} \qquad (2)$$

$\gamma_{des}(t)$ represents the amount of desorption per unit time and $\gamma_{\text{¿}\text{¿}(t)\text{¿}}$ indicates the amount of adsorption per time. n_{max} represents the maximum value of physical amount attached to the surface. Since$\gamma_{des}(t)$ and $\gamma_{\text{¿}\text{¿}(t)\text{¿}}$ are not constant and depend on the gas pressure, so they made the following relationship as a model.

$$\gamma_{\text{¿}\text{¿}=\alpha_{\text{¿}\text{¿}\text{¿}\text{¿}\text{¿}}} \quad (3)$$

$$\gamma_{des}=\alpha_{des}\left(g_{mn}^{des}-g_{mn}\right)P+g_{mx} \quad (4)$$

where $g_{mx}^{\text{¿}\text{¿}\text{¿}}$ and g_{mn}^{des} represent the range of pressure and $\alpha_{\text{¿}\text{¿}\text{¿}}$ and α_{des} are coefficient fitted to experimental data. Using the model equations (1) to (4), the relationship between the excitation time and the emission intensity is plotted in Figure2.11. It can be seen that the model has a similar curve to the time variation of the pressure obtained from the experiments.

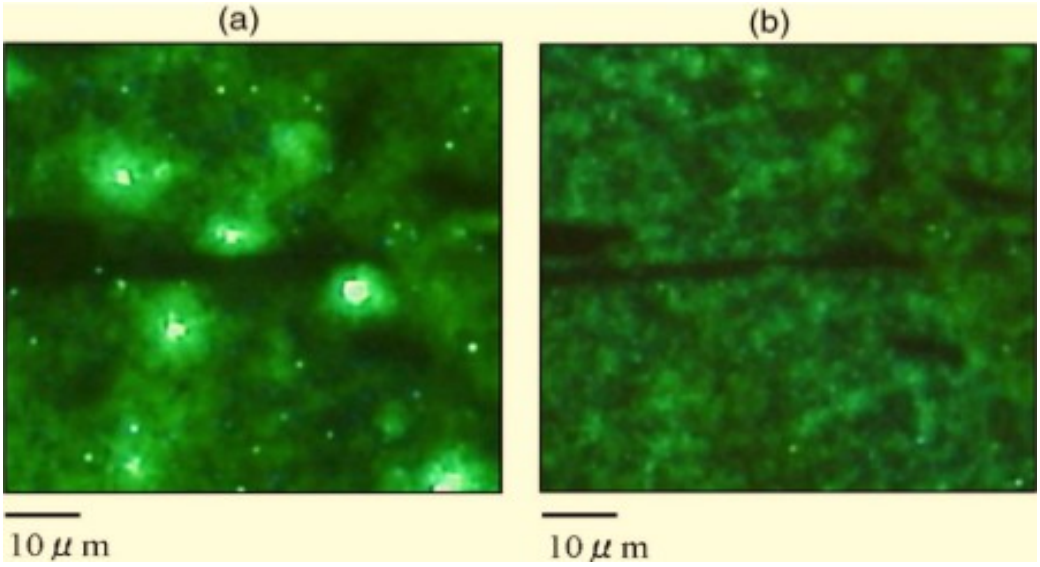

Figure2.4 Blinking phenomena of an InGaN/GaN SQW with a luminescence wavelength of 510nm. (a) is at an excitation wavelength of 365nm and (b) is at 405nm. Blinking appears easily in (a), while no blinking occurs in (b) when only the quantum well layer is excited. [9]

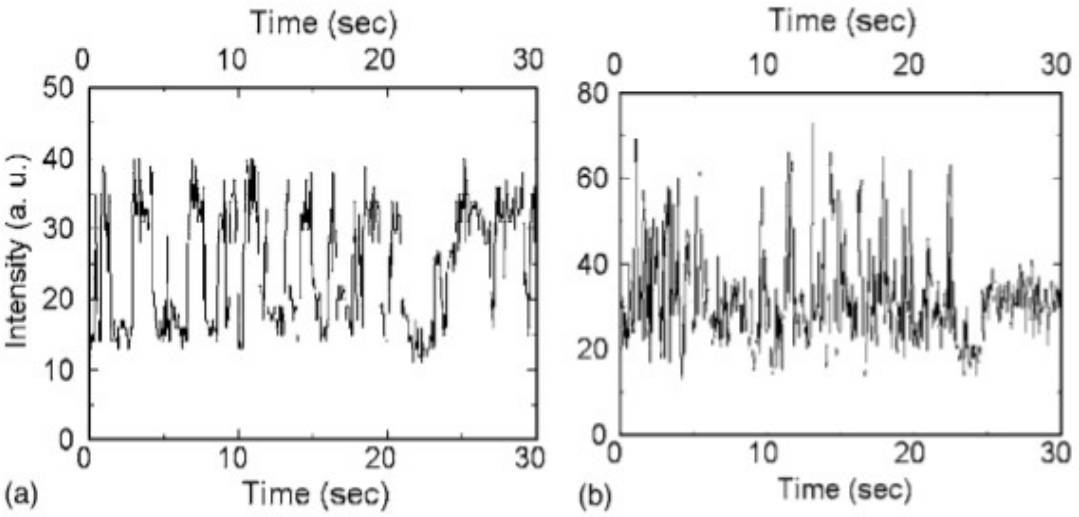

Figure2.5 InGaN/GaN SQW has two types of Blinking, one that moves back and forth between the two intensities, as in (a), and the other, chaotic blinking via all values, as in (b). [9]

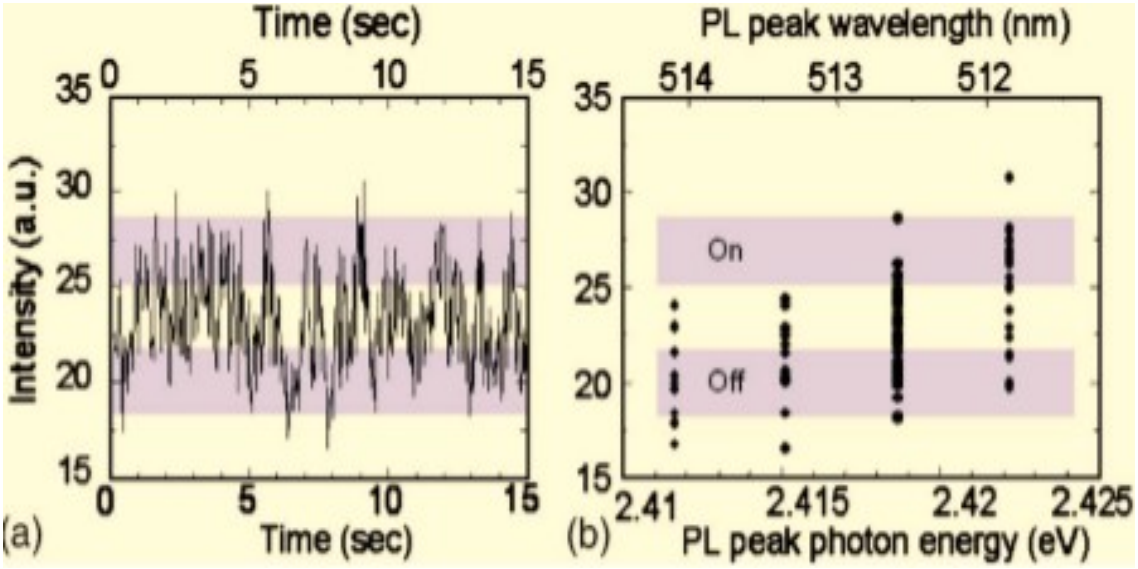

Figure2.6 (a) Time-series data of the luminescence intensity of the InGaN/GaN SQW blinking phenomena: (b) Relationship between peak wavelength and luminescence intensity. [9]

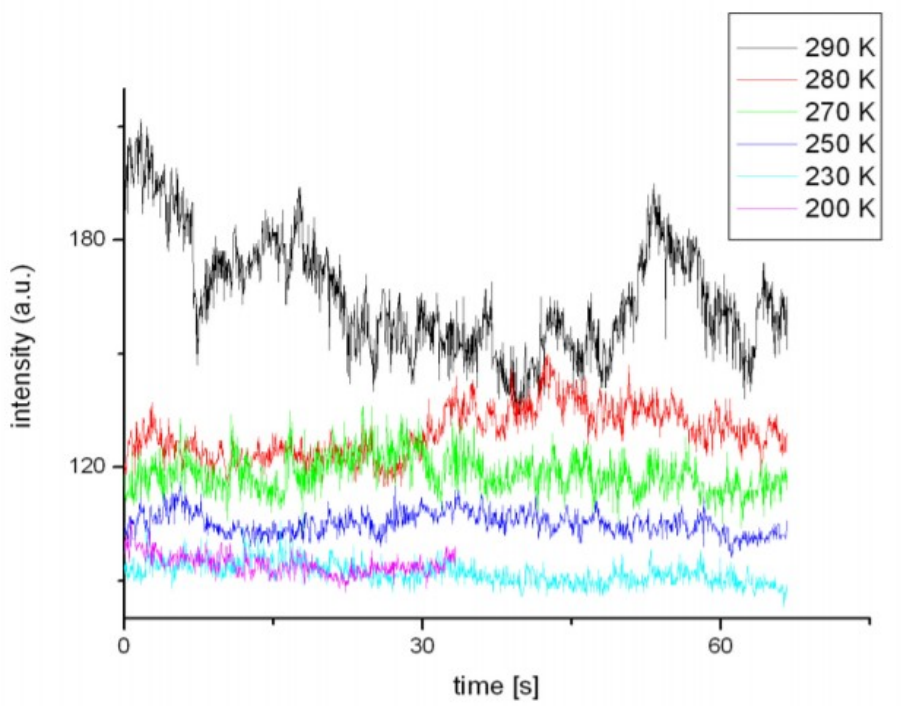

Figure2.7 Time-series variation of blinking intensity at different temperatures [9]

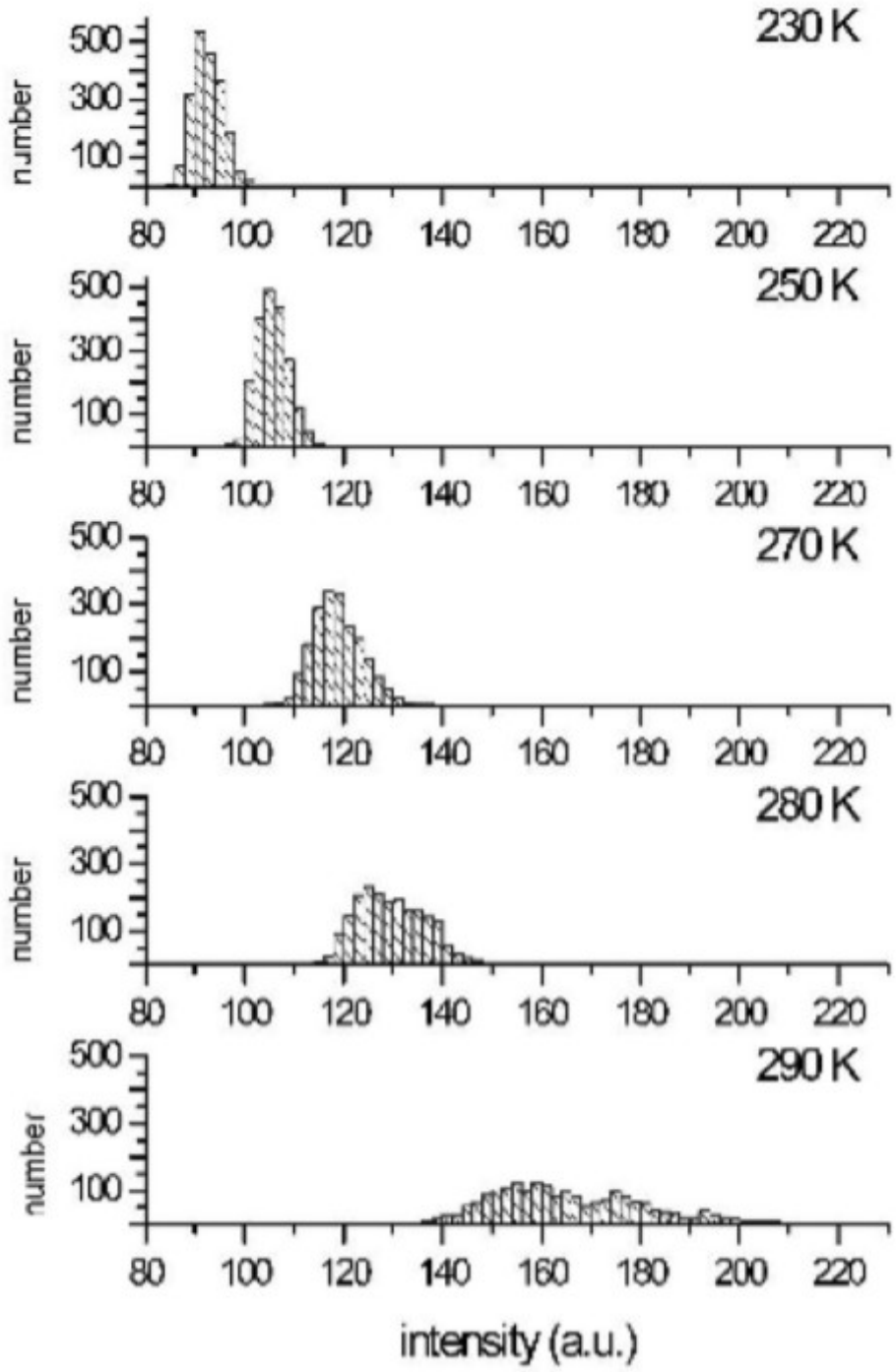

Figure2.8 Histogram of the blinking intensity at each temperature [9]

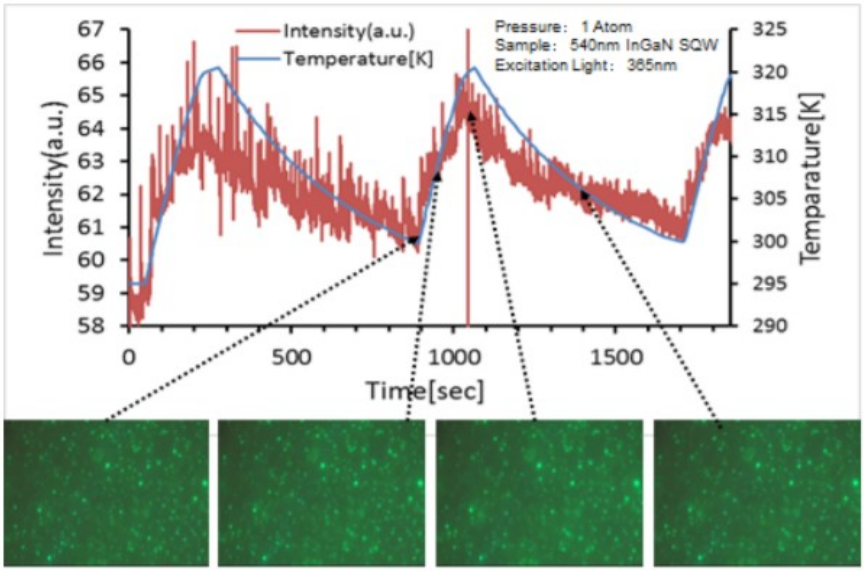

Figure2.9 The temperature dependence of the surface luminescence of InGaN/GaN SQW with a luminescence wavelength of 540nm irradiated with 365nm excitation light. The blue and red lines show temperature and intensity changes, respectively. [17]

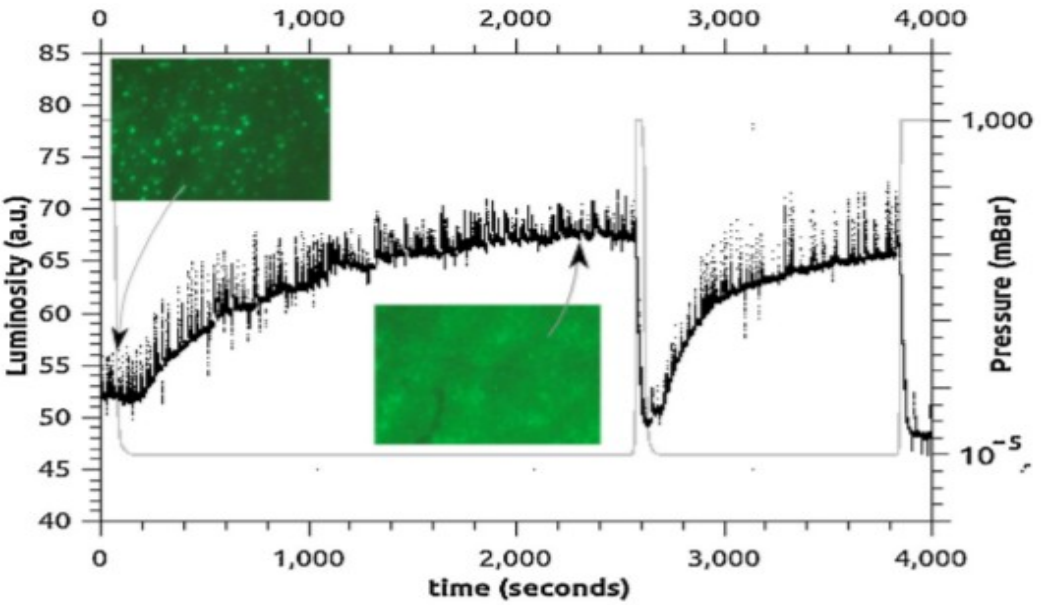

Figure2.10 The pressure dependence of the surface luminescence of InGaN/GaN SQW with a luminescence wavelength of 540nm irradiated with 365nm excitation light [18]

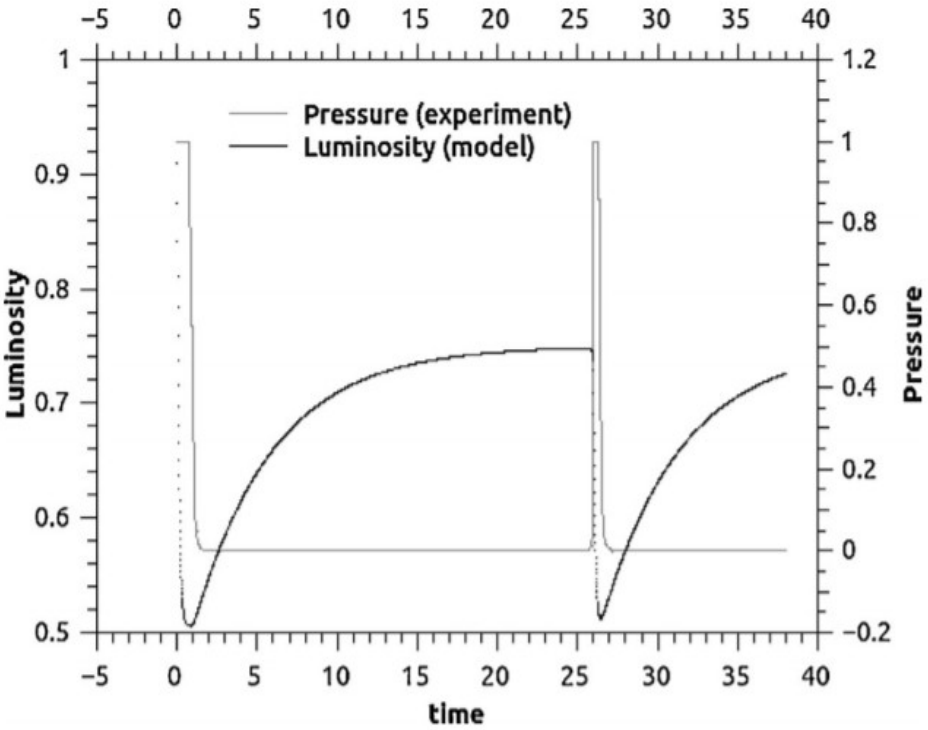

Figure2.11 Time series data of the experimental pressure variation and the modeled luminescence intensity [18]

3 Samples and measuring systems

3.1 Samples

Samples I used in this study are shown in Figure3.1. These were provided by Prof. Yoichi Kawakami of Kyoto University and Nichia Corporation, and are the same as those used by T.Tsutsumi, who completed his studies in our laboratory five years ago. The double heterostructure consists of a 4μm GaN layer, a 3nm InGaN layer, and a 5nm GaN layer grown in the [0001] direction on the sapphire substrate in that order. The growth method used was the metallic organic vapor deposition method, and no doping was applied to any of the layers in the sample. As noted in Chapter 1, the emission wavelength can be changed by changing the indium composition ratio x. In this study, I used samples with emission wavelengths of 460nm and 510nm.

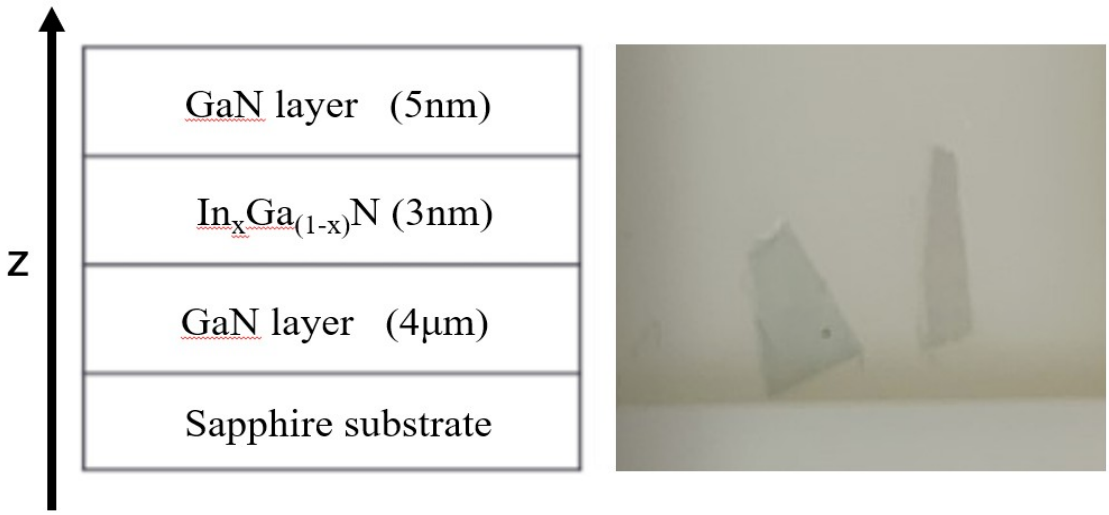

Figure3.1 Structure and photographs of the InGaN/GaN SQW used in this study

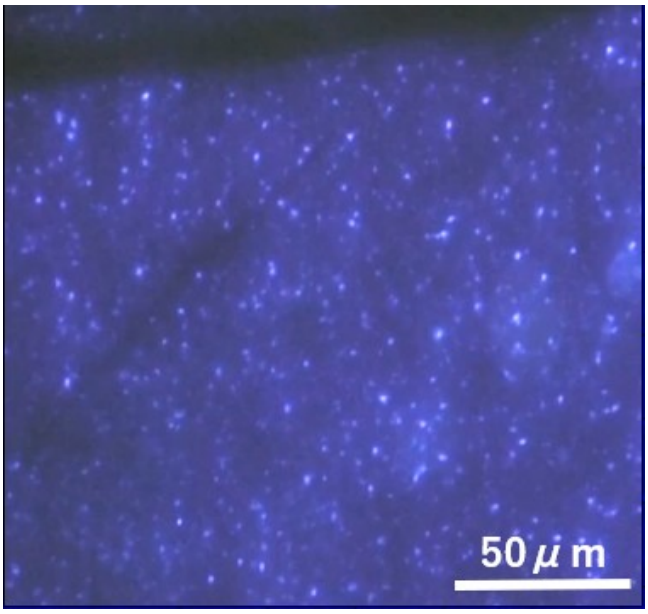

Figure3.2 Blinking phenomena observed at an emission wavelength of 460nm

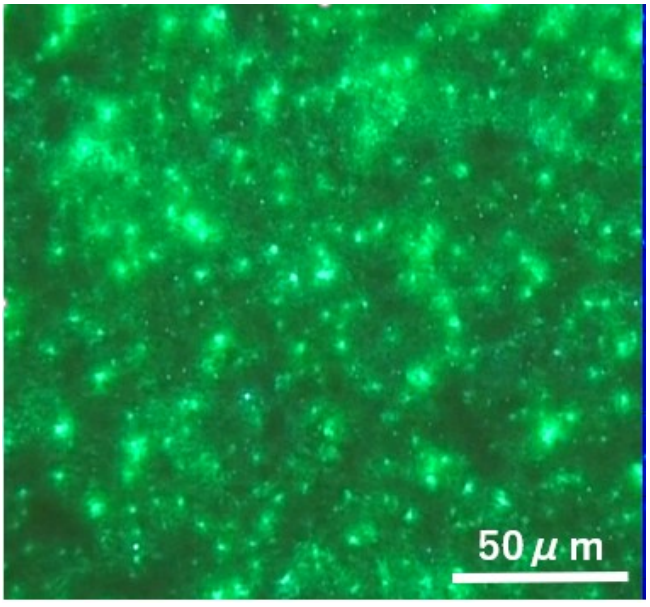

Figure3.3 Blinking phenomena observed at an emission wavelength of 510nm. The blinking points tend to be larger than that of the 460nm sample.

3.2 Selective excitation fluorescence microscope

A schematic diagram of the selective excitation fluorescence microscope used in this study are shown in Figure3.4. The microscope is an Olympus BX51WI-33FL-YS2, and the mercury lamp used as a light source is an Ushio BC2078 5000273 100W USH-102D. The light from the mercury lamp passes through an excitation filter, which allows only the excitation wavelength to be transmitted. Excitation light is irradiated onto the sample and fluorescence and excitation light are emitted. By passing through the absorption filter, the excitation light is reflected and only the fluorescence wavelengths are transmitted to our eyes. The combination of the excitation filter and the absorption filter determines the method of excitation. The combination of filters can be selected from the mirror unit on the microscope. We have five different mirror units in our laboratory: BFL, NU, NBV, NIBA and WIG. The spectra of excitation and fluorescence wavelengths that can be transmitted by each unit are shown below. This figure was provided to us by Olympus. Blinking is generated by taking out the wavelength of 365nm only in the mercury lamp and using it as an excitation light. In addition, as mentioned earlier, since the fluorescence wavelengths of 460nm and 510nm are observed, the necessary mirror unit for observing the blinking is NU, and the blinking does not occur under the conditions of mirror units other than NU. The blinking is observed with the 3CCD camera (HDR-SR1, SONY) mounted on the top of the microscope, which has a magnification of 10x and the objective lens is set to 50x, so the blinking is observed with a total of 500x magnification. The resulting video data is 1440 pixels by 1088 pixels with a frame rate of 30fps. By processing this recorded data by programming, it is possible to perform statistical analysis.

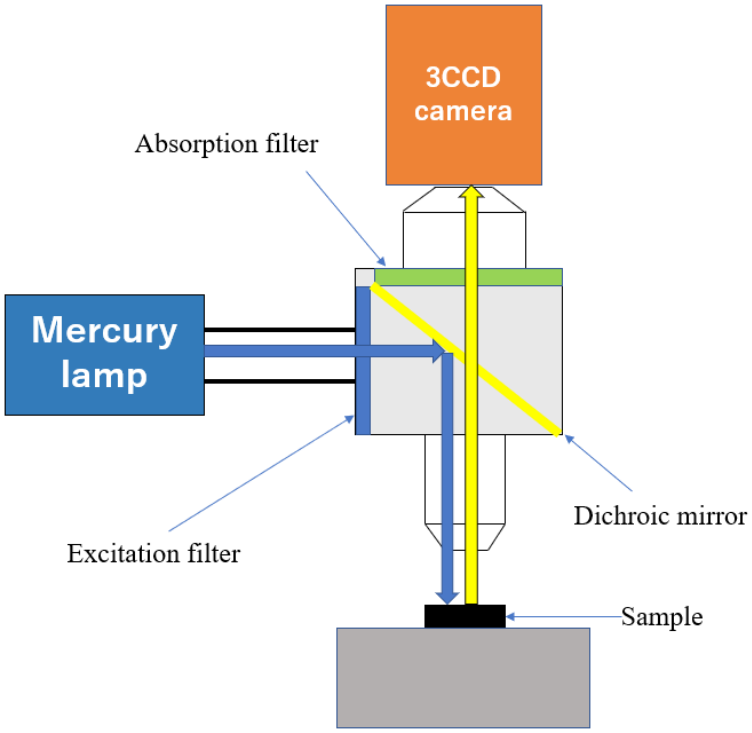

Figure3.4 Diagram of the selective excitation fluorescence microscope

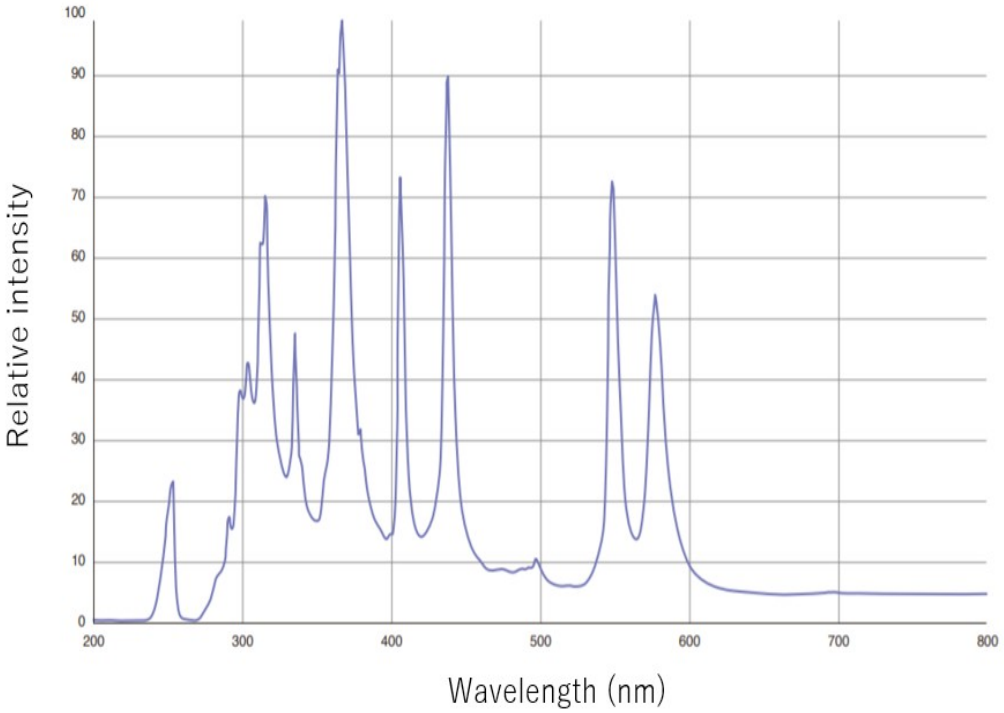

Figure3.5 Spectral distribution of the mercury lamps used in this study (I modified) [19] (https://www.ushio.co.jp/documents/products/light_source/USH102D_J.pdf)

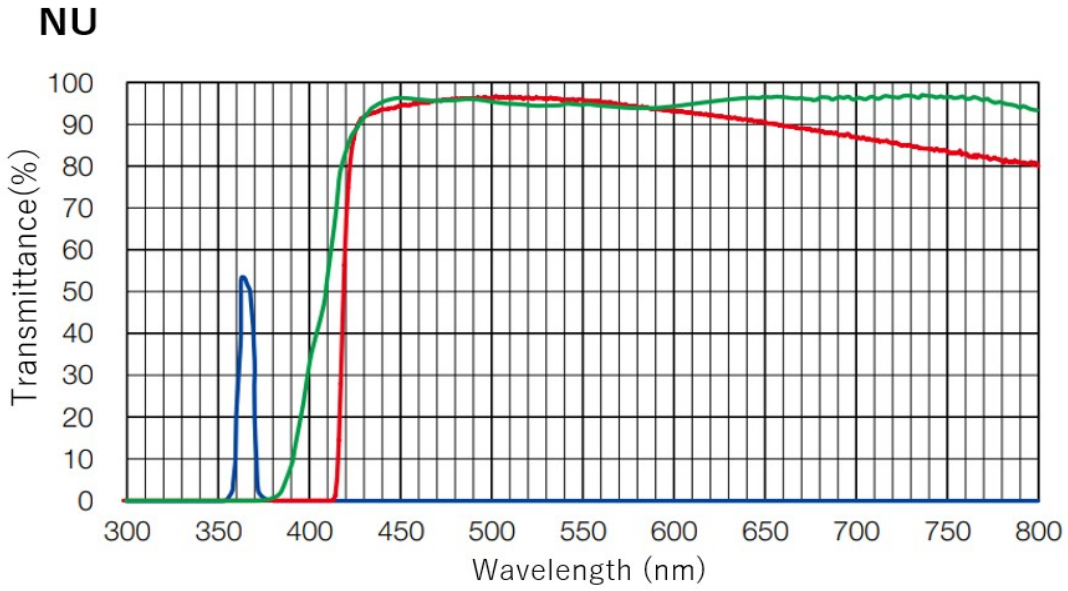

Figure3.6 The spectra of excitation and fluorescence wavelengths that can be transmitted by NU. The blue line indicates the excitation filter, the red line indicates the absorption filter, and the green line indicates the dichroic mirror [20]

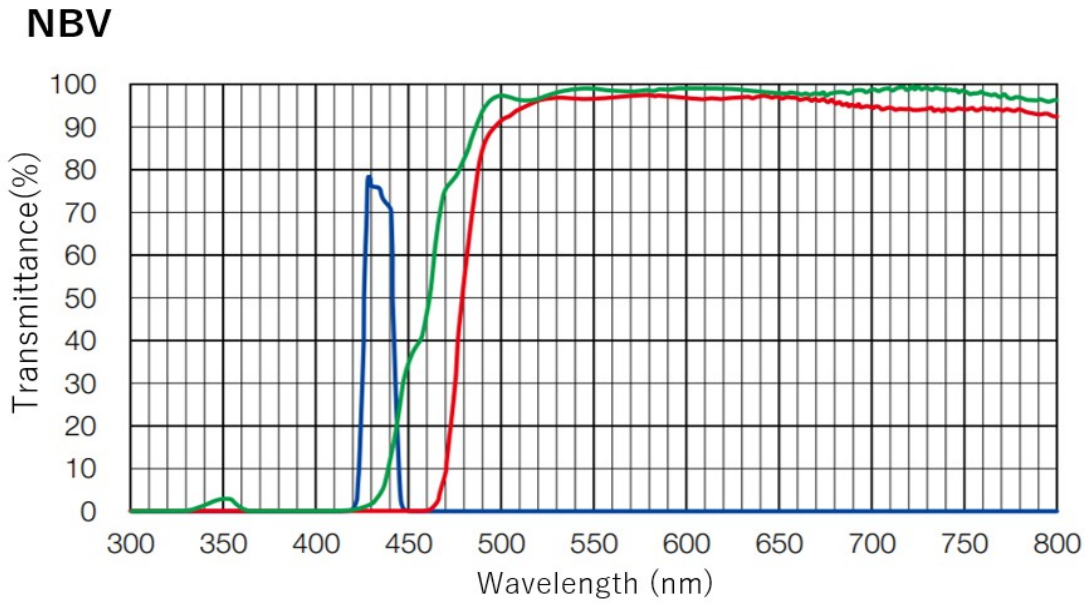

Figure3.7 The spectra of excitation and fluorescence wavelengths that can be transmitted by NBV [20]

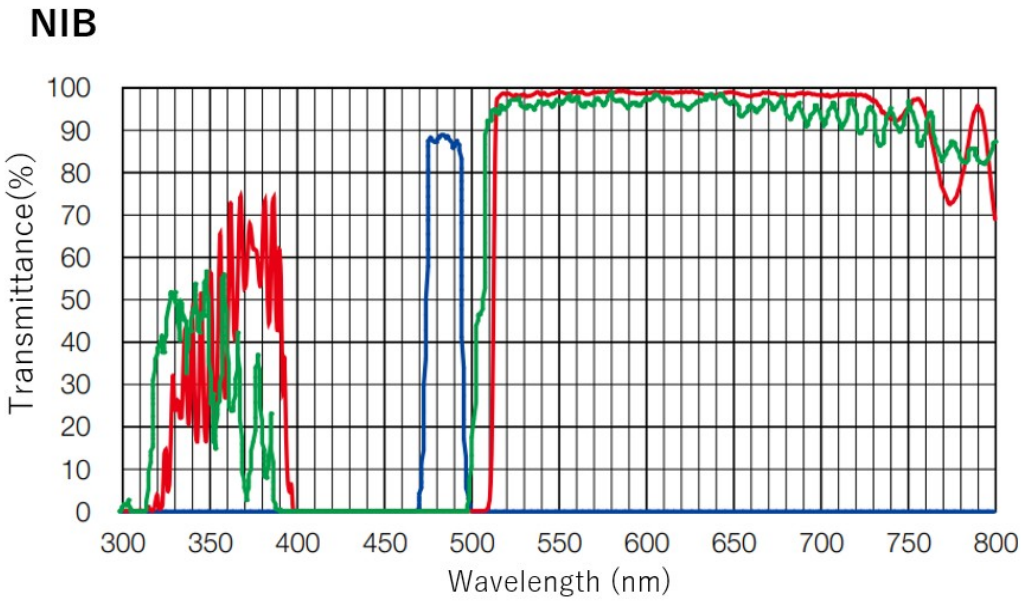

Figure3.8 The spectra of excitation and fluorescence wavelengths that can be transmitted by NBV [20]

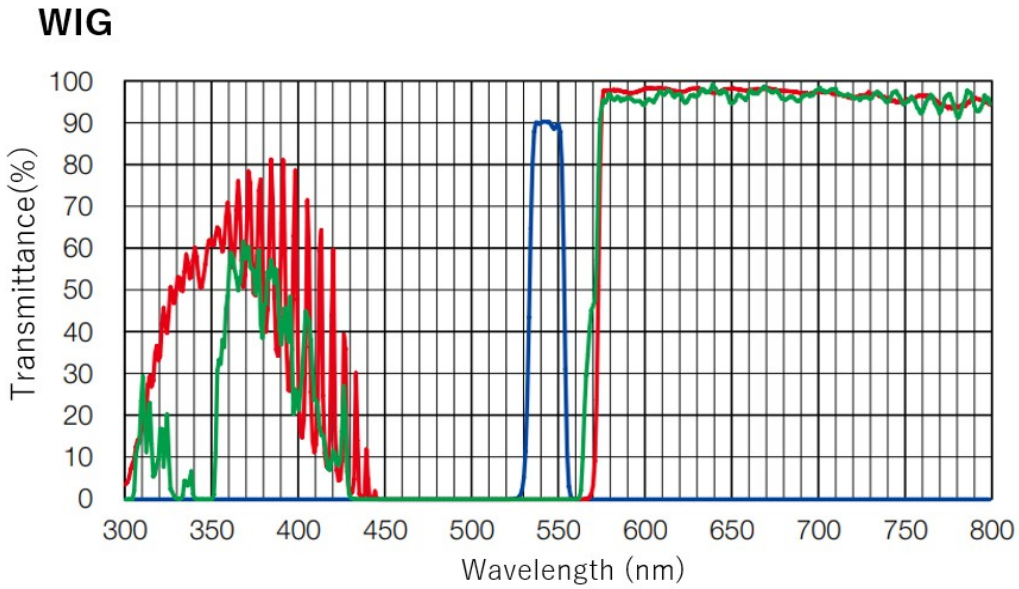

Figure3.9 The spectra of excitation and fluorescence wavelengths that can be transmitted by WIG [20]

3.3 Video data processing methods (quantification)

Directly obtained blinking video data is relatively large in size and contains noise. I used Avidemux 2.7(Qt 5) to crop and remove noise to reduce the size of the video. The optical

intensity of the time series can be obtained by calculating and integrating the optical intensity at each frame. In addition, since it can be expressed in terms of 8-bit emission intensity, the optical intensity per pixel is calculated by calculating the brightness (0-255) in red, green, and blue, respectively, as shown in equation (1), and averaging them. It is also possible to calculate the overall intensity by specifying an area instead of a pixel unit as in equation (2).

$$I(t)=\frac{R(t)}{3}+\frac{G(t)}{3}+\frac{B(t)}{3} \qquad (1)$$

$$I(t)=\sum_{x=x1}^{x2}\sum_{y=y1}^{y2}\frac{R(x,y,t)+G(x,y,t)+B(x,y,t)}{3(x2-x1)(y2-y1)} \qquad (2)$$

Although I do not directly measure the spectral intensity of the blinking, the image analysis as shown above allows us to analyze the time variation of the optical intensity of the blinking and other statistical analysis.

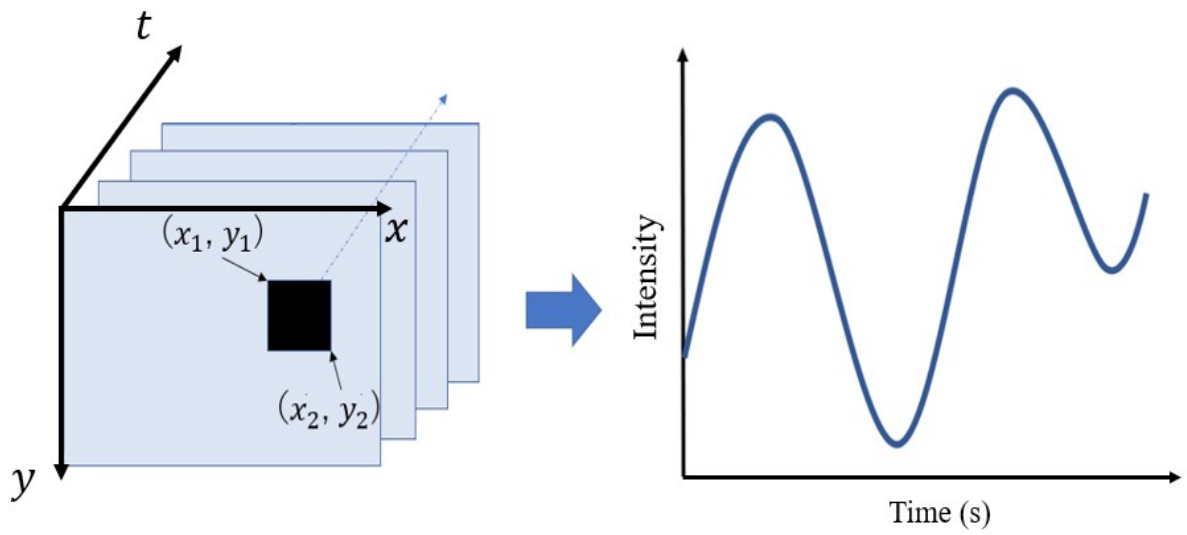

Figure3.10 The video data processing method is represented as a diagram. By recording the coordinates (x_1, y_1) of the upper left part and (x_2, y_2) of the lower right part of the area where we want to measure the intensity, and applying equation (2) described on the previous page, we can arrange the intensity for each frame in chronological order, resulting in a time series graph like the one on the right. Also, since this is a video data processing, it is an image coordinate system.

4 Temperature dependence of blinking phenomena

4.1 Introduction

As mentioned in Chapter 2, the temperature dependence of InGaN/GaN SQW has been studied in the past. However, there has been no quantitative discussion of how the blinking points behave in response to large temperature changes. Here, I used InGaN/GaN SQW with emission center wavelengths of 460nm and 510nm to study the behavior of the blinking point from 300K to 373K at 10K intervals.

4.2 Experimental method

I measured the temperature dependence of the blinking phenomena. The temperature dependence of the blinking phenomena can be measured by placing InGaN/GaN SQW on a heater attached to a temperature controller and adjusting the temperature controller. The temperature controller used was Cryogenic Control System's Model 32. After the temperature displayed on the temperature controller was kept constant, the shutter on the microscope was opened and the excitation light was irradiated for 30 seconds in order to make the comparison under the same conditions as possible. The temperature was measured in two ways: from lower to higher and from higher to lower. The blinking phenomena was captured on a 3CCD camera mounted on top of the microscope. The spatial distribution of the blinking points was calculated by analyzing the video data. This method of image analysis is also described in Chapter 3. To quantify the blinking phenomena, I created a standard deviation map. The standard deviation map allows us to show the blinking area quantitatively. More intense blinking areas result in higher standard deviation values and weaker blinking areas result in lower standard deviation values.

4.3 Experimental result

The standard deviation map for each temperature is shown in Figure4.1. This is the result of irradiating InGaN/GaN SQW with an emission wavelength of 460nm with excitation light of 365nm. From the standard deviation map, it is clear that blinking is most active at low temperature environment, but it can be seen that the intensity of blinking tends to be relieved by increasing temperature. At the maximum temperature of 373K, the intensity of blinking was most moderated, and more than 90% of blinking points disappeared. This result is clear not only on the standard deviation map but also visually.

Figure4.2 is the result of irradiating InGaN/GaN SQW with an emission wavelength of 510nm with excitation light of 365nm. Similar to InGaN/GaN SQW with an emission wavelength of 460nm, it can be seen that the blinking becomes most intense in a low temperature environment, and the intensity of blinking points tend to be relieved as the temperature rises. However, unlike the 460nm InGaN/GaN SQW, blinking was still present even at the maximum temperature of 373K. This result is also visible visually as well as the standard deviation map.

Furthermore, when comparing the standard deviation values of both samples, the result is higher for InGaN/GaN SQW at 510nm. This standard deviation value is based on the temperature that the blinking was most intense, and the color bar is created. In other words, it means that the InGaN/GaN SQW having an emission wavelength of 460nm blinks more rapidly than the InGaN/GaN SQW having an emission wavelength of 510nm. As reported by C. Feldmeier, 460nm InGaN/GaN SQW is less prone to blinking points than 510nm InGaN/GaN SQW.[3] Same result was obtained in this study, and it was found that the more likely the sample to blink, the greater the intensity of the blinking.

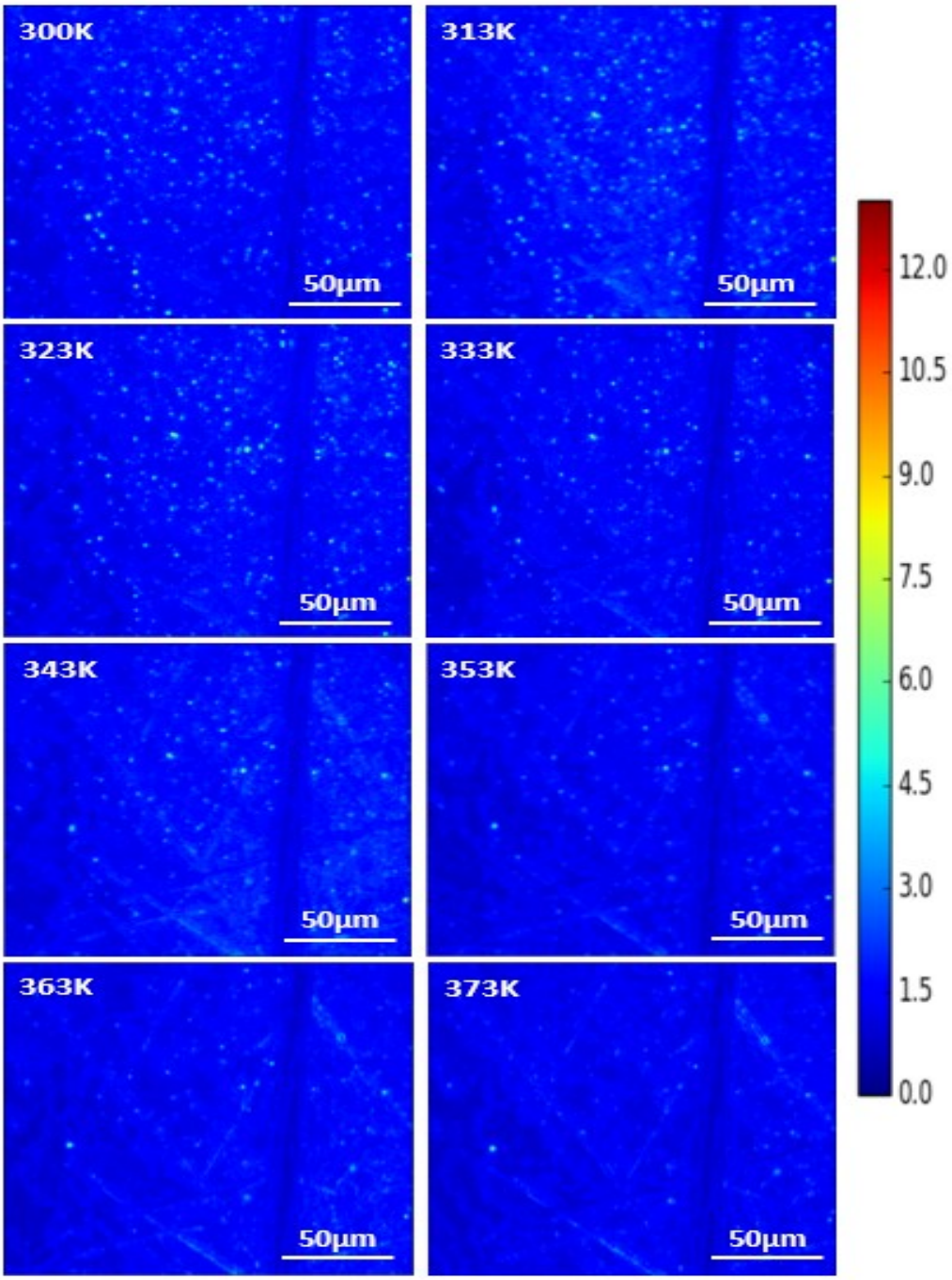

Figure4.1 I created a standard deviation map to quantify the blinking phenomena. This is the standard deviation map for each temperature, and is the result for an InGaN/GaN SQW with an emission wavelength of 460nm. The larger the value, the more intense the blinking.

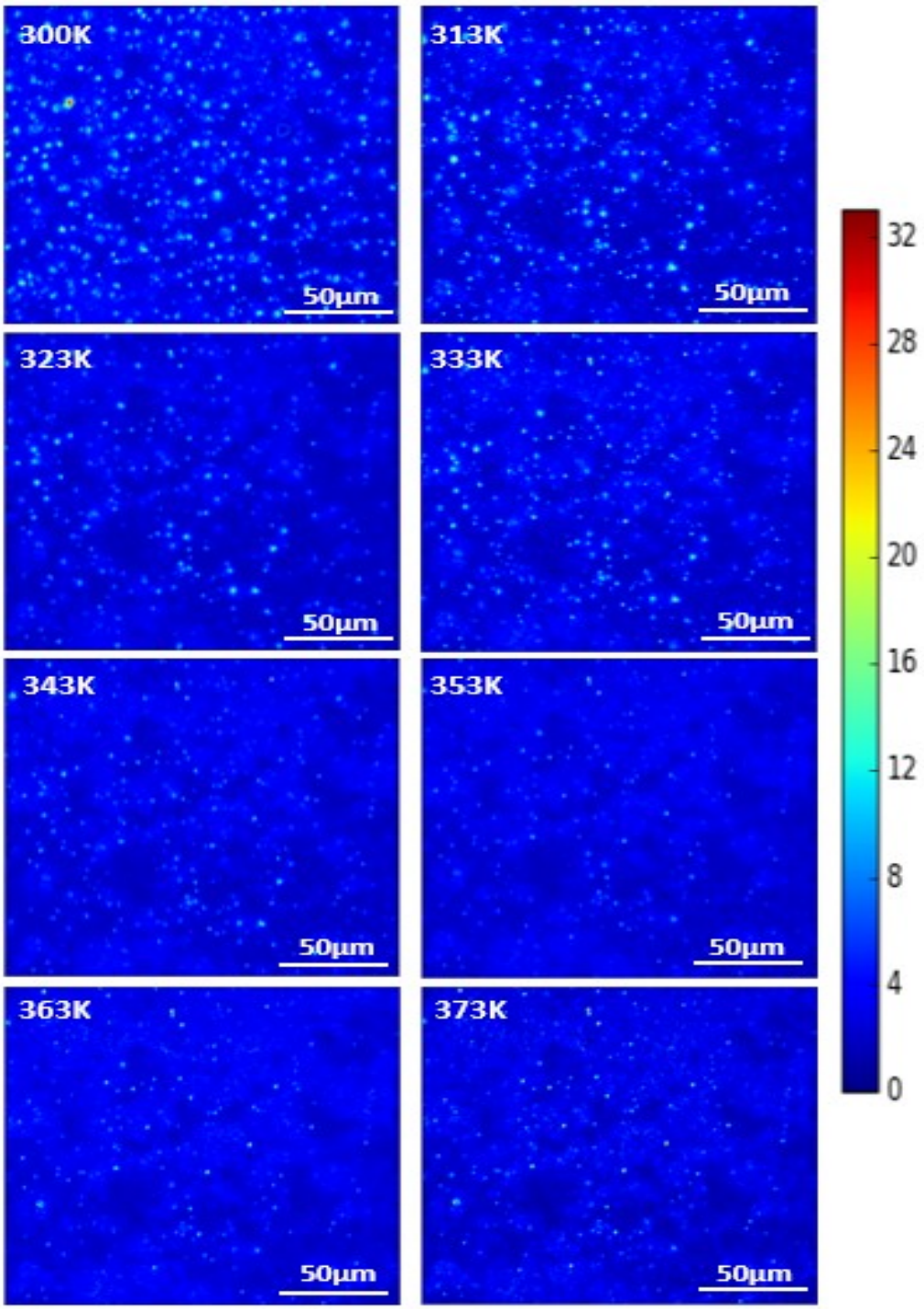

Figure4.2 The standard deviation map is the same as in Figure4.1. This is the result of an InGaN/GaN SQW with an emission wavelength of 510nm.

4.4 Discussion

It was found that blinking behavior changed significantly with temperature changes, and that when excited in a relatively low temperature environment, blinking was most likely to be active in both samples. According to the Figure4.1 and Figure4.2, it can be seen that the blinking points gradually decrease as the temperature rises, and the blinking disappeared on the 460nm sample, but the blinking was still present even at the maximum temperature of 373K on the 510nm sample. However, depending on the location, there was an area where the blinking gradually decreased every 10K, and there was an area where the blinking increased at 10K or 20K and then decreased after that. The cause of this has not been identified. However, there was a common case that blinking was likely to occur in a relatively low temperature range, and blinking was unlikely to occur in a high temperature range. Furthermore, in the 460nm sample, the blinking almost disappeared at the maximum temperature of 373K, and in the 510nm sample, the blinking was present even at 373K. Since the only difference between the two is the indium content, it is thought that the cause is that there are many defects due to the difference in the indium content.

It is considered that the coefficient of thermal expansion increased and the distortion inside the crystal increased as a factor of the decrease of the blinking point when the temperature rise. The carriers required for recombination are more likely to be trapped by larger defects and can result in non-radiative recombination that emits heat rather than light. Another factor may be reduced electron mobility, but the study could not determine the exact factor because various physical quantities change with temperature.

5 Change in blinking phenomena due to liquid adhesion

5.1 Introduction

As mentioned in Chapter 2, the luminescence change phenomena were caused by the vacuum change, suggesting that surface deposits are involved in the luminescence and blinking. Therefore, I studied how the blinking phenomena changes when the liquid is deposited on the surface.

5.2 Experimental method

I used InGaN/GaN SQW with an emission wavelength of 460nm and InGaN/GaN SQW with an emission wavelength of 510nm. I deposited a liquid on the surface of the sample before excitation with light. I covered the surface with a cover glass after depositing it so that the liquid is uniformly distributed. Since the transmittance of the cover glass is almost 100%, I do not expect it to have much effect on the observation of the blinking phenomena. The liquids used in this study are water and ethanol and I excited the sample for 30 seconds. To quantify the blinking phenomena, I made a standard deviation map as well as the temperature dependence.

5.3 Experimental result

The results of the experiment showed that the behavior of blinking varied greatly depending on the liquid deposited on the surface. Figure5.1 shows the standard deviation map for InGaN/GaN SQW with an emission wavelength of 460nm, and Figure5.2 shows the standard deviation map for InGaN/GaN SQW with an emission wavelength of 510nm. The same results were obtained for both samples, indicating that the blinking point is induced by the adhesion of liquid. The blinking is weakest when nothing is attached to the surface, and the intensity of the blinking increases slightly when water is attached. When ethanol adhered to the surface, the blinking became incredibly intense. I quantified the blink phenomena with a standard deviation map, and the actual visual observation shows that the change in blinking behavior due to liquid adhesion is remarkable. I also performed the experiment with different excitation locations and obtained similar results.

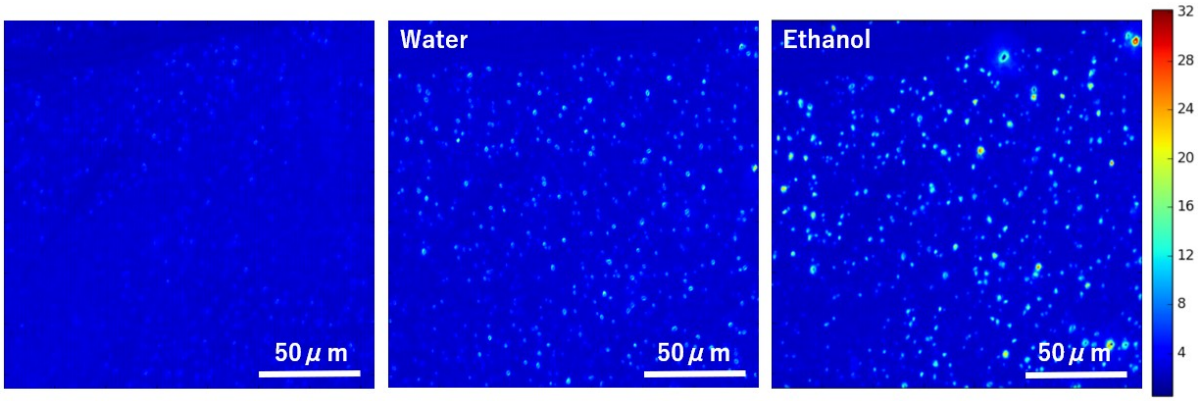

Figure5.1 A standard deviation map for each liquid adhesion. The sample is an InGaN/GaN SQW with an emission wavelength of 460nm. It can be seen that the blinking is especially intense for ethanol adhesion.

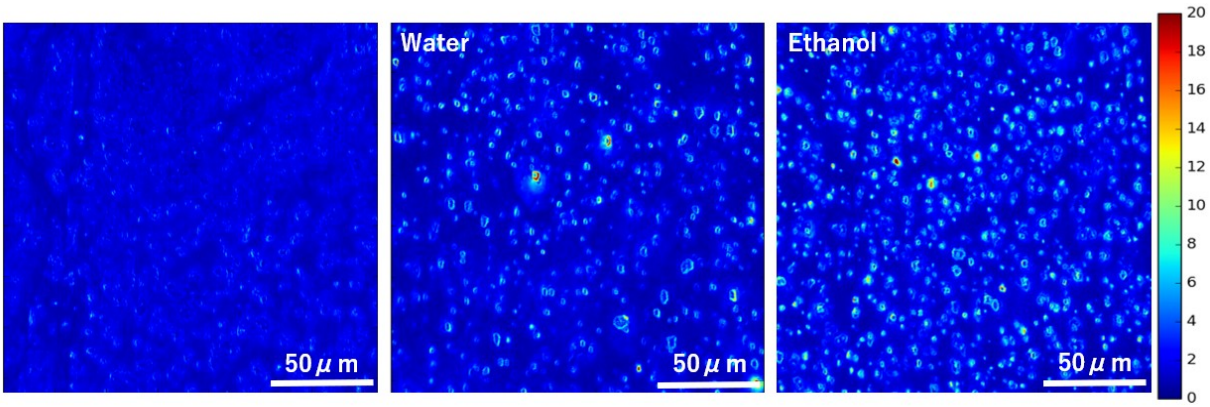

Figure5.2 A standard deviation map for each liquid adhesion. The sample is an InGaN/GaN SQW with an emission wavelength of 510nm. It can be seen that the blinking is especially intense for ethanol adhesion.

5.4 Discussion

It was found that the blinking phenomena was induced by the adhesion of the liquid and that the behavior of the blinking points differed depending on the liquid type. This suggests that the adsorbed material on the surface plays an important role in the blinking phenomena. The blinking is thought to be caused by the QCSE as described in Chapter 2. If the overlap of

the wavefunctions increases and decreases at high speed, the blinking is expected to be more intense. If the magnitude of the piezoelectric field is constantly changing over time, the above phenomena is likely to occur. The optical intensity of the blinking also increased, so it is also suggested that the adsorbent increases the density of states near the valence band, creating an environment in which many electrons can be excited at once, and increasing the recombination rate of carriers.

6 Statistical analysis of the blinking phenomena

6.1 Consideration of how the blinking point glow using Standard Deviation map

The blinking phenomenon can be quantified by expressing it as a standard deviation map. By enlarging the blinking points displayed on the standard deviation map, we can see the distribution of the variation in optical intensity over the measurement time of a single blinking point. When we took out the blinking points and examined them one by one, we found that there are several types of blinking points, and their blinking patterns are different. Figure6 shows the blinking patterns that were particularly conspicuous. Figure6.1(a) shows a pattern of two blinking points blinking significantly, Figure6.1(b) shows a donut-shaped pattern where the center of the blinking point hardly blinks but the surrounding area blinks significantly, Figure6.1(c) shows a pattern where the center of the blinking point blinks significantly, and finally Figure6.1(d) shows that the intensity of blinking is a uniform pattern. Since the maximum standard deviation differs for each blinking point, the standard deviation is normalized.

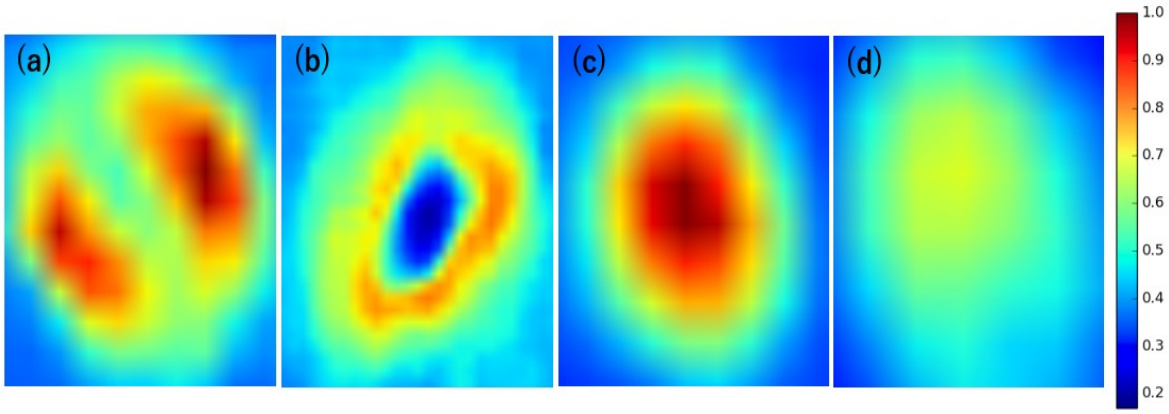

Figure6.1 Enlarging the standard deviation map, the above blinking pattern is conspicuous

6.2 Correlation between blinking points

As shown in Figure6.1(a), I report a very interesting feature of the blinking point where the intensity varies significantly between two locations. In particular, I cut out one pixel in a region with a high standard deviation and calculated its correlation with another region with a high standard deviation. The correlation here refers to the correlation of optical intensities in the time series. As shown in Figure6.2, the correlation was relatively strong and negative. There were some blinking points of weak correlation, but the result was definitely negative. This means that when the optical intensity of one become higher, the intensity of the other become lower, which occurs every one frame (0.03 seconds). Although it is not possible to include all the blinking data in this paper, Figure6.3 shows a plot of the correlation between the two regions where the optical intensities show a negative correlation. It is also clear from this correlation that the two regions are negatively correlated with each other.

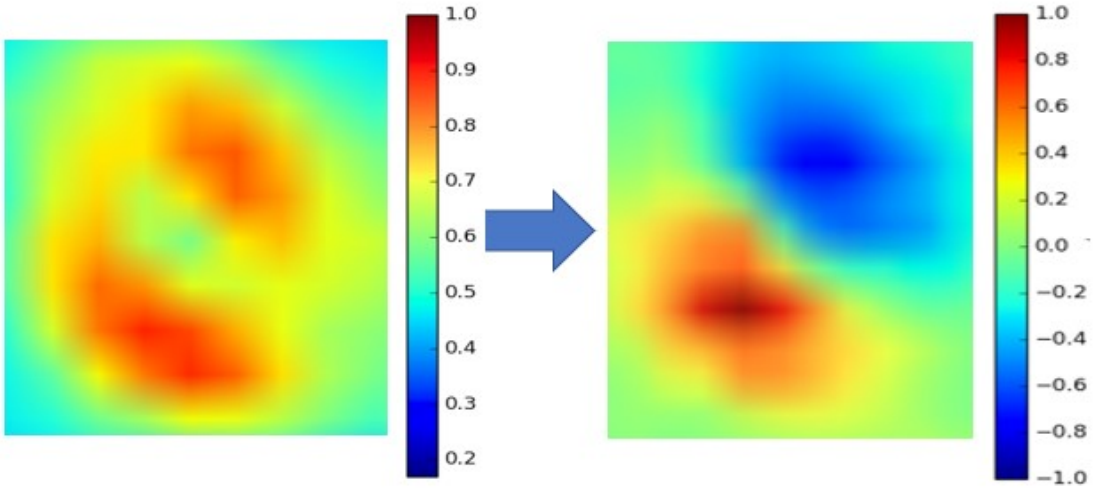

Figure6.2 Cut out a single pixel with a high standard deviation value and transformed it into a correlation distribution of intensities for that location. This data is just one example among many blinking points.

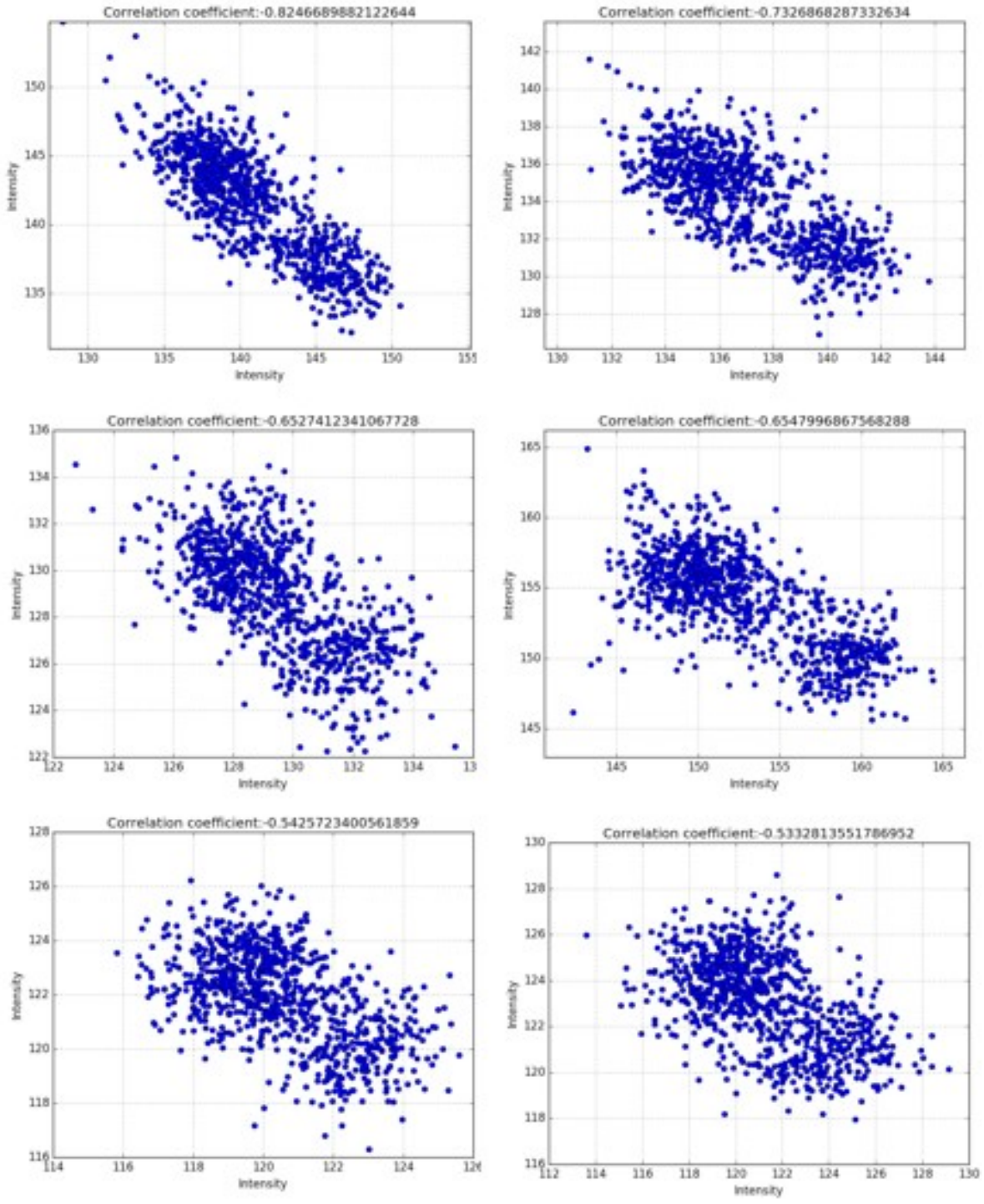

Figure6.3 Correlation diagram of two regions where optical intensities are negatively correlated. It is not possible to put all the blinking data, so the data of six blinking points are shown. Correlation coefficients are also shown.

The data on the previous page shows the correlation for a single blinking point. Thus, I have also performed extensive correlation mapping for a single pixel. Similarly, I picked out the blinking points in Figure6.1(a) that had a particularly high standard deviation, and calculated the overall correlation for those points. The result is shown in Figure6.4 and Figure6.5. From these results, we can see that there is a correlation not only between one of the blinking points, but also between other blinking points that exist in the surrounding. It is also apparent that there are multiple points consisting of two regions with negative correlations. As shown in Figure6.1, there are various ways to blink, but as a result of the above approach, I found that blinking points other than (a) also tend to consist of two blink regions with negative correlation. Even for such blinking points, the correlation diagram was plotted, and a negative correlation with a downward slope as shown in Figure6.3 could be obtained.

Figure6.4 and Figure6.5 show that almost all blinking points consist of two negatively correlated regions. I selected other blinking points that were negatively correlated with each other and measured their optical intensity in the same time series. The results are shown in Figure6.6 and Figure6.7. These data show that the blinking points behave as if they were in sync with each other. Two seconds after the start of measurement, the blinking optical intensity of A (G), B (H), and C (I) increases, and processing takes about 23 seconds. In contrast, blinking D (J), E (K), and F (L) work in contrasting ways. That is, not only the optical intensity shows a negative correlation for each frame (0.03 seconds), but also the optical intensity shows a negative correlation even when considered on a long-time scale. At the same time, the optical intensity in the surrounding non-blinking area was also measured, but there was no characteristic increase or decrease in light intensity as shown in the graph, and there was no sign of synchronization, Thus, I think this is not due to noise or light sources.

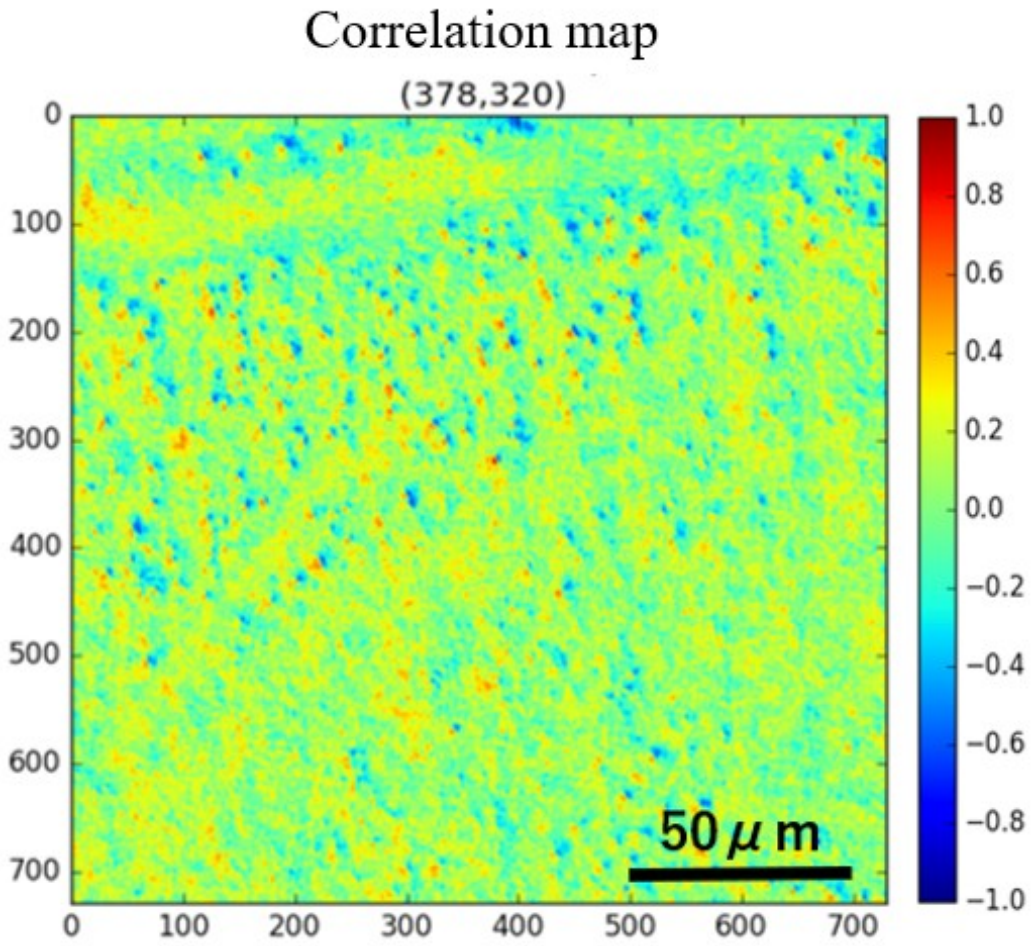

Figure6.4 The correlations shown in Figure6.2 have been transformed into an extensive correlation mapping, showing that there is correlation not only in one blinking point, but also in others present in the surroundings. There are also many points that consist of two blinking regions with negative correlation. The data is based on (378,320) pixels.

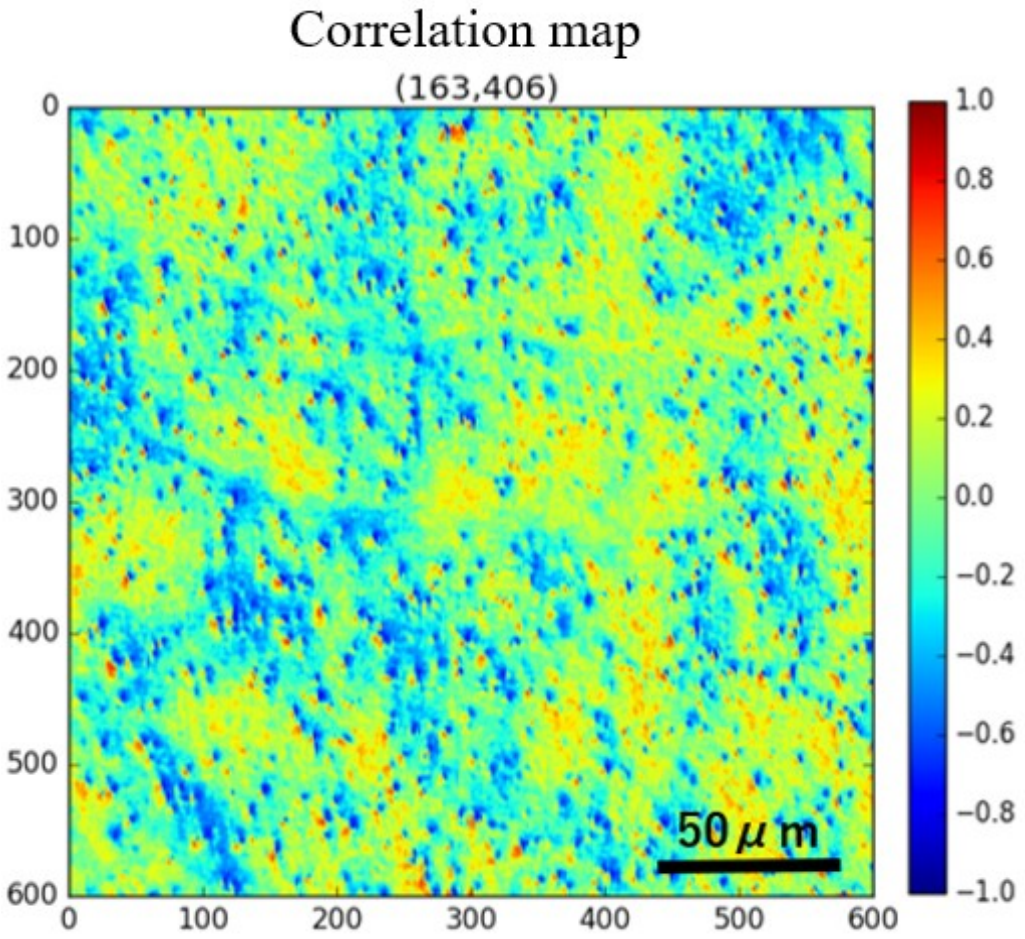

Figure6.5 Correlation mapping as in Figure6.4. The results are measured in a different region. This map also shows that the blinking consists of two regions with negative correlation. The data is based on (163,406) pixels.

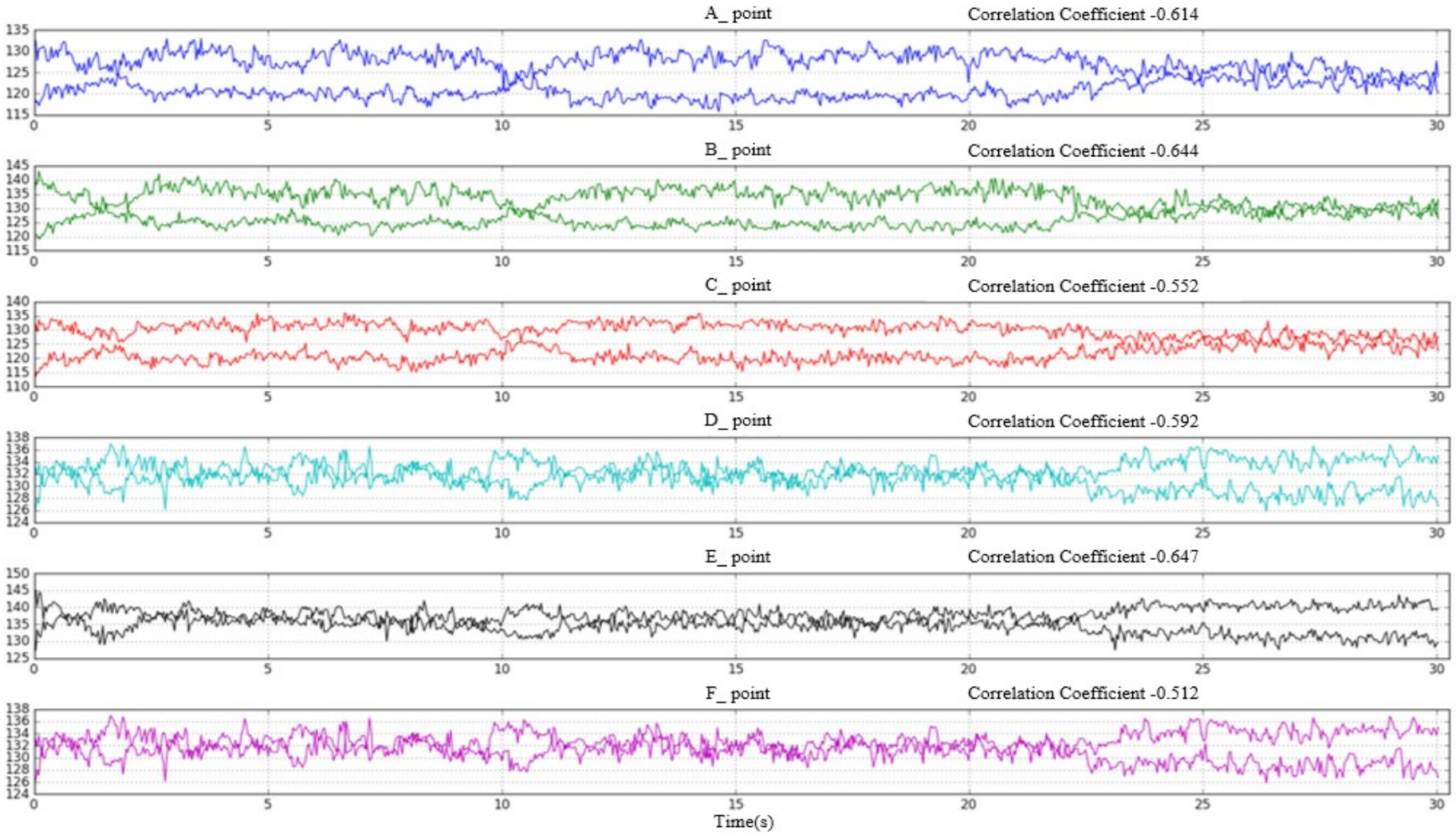
A_ point
Correlation Coefficient -0.614
B_ point
Correlation Coefficient -0.644
C_ point
Correlation Coefficient -0.552
D_ point
Correlation Coefficient -0.592
E_ point
Correlation Coefficient -0.647
F_ point
Correlation Coefficient -0.512
Time(s)

Figure6.6 Time series optical intensity of two regions composed of negatively correlated. These data are spatially different blinking points.

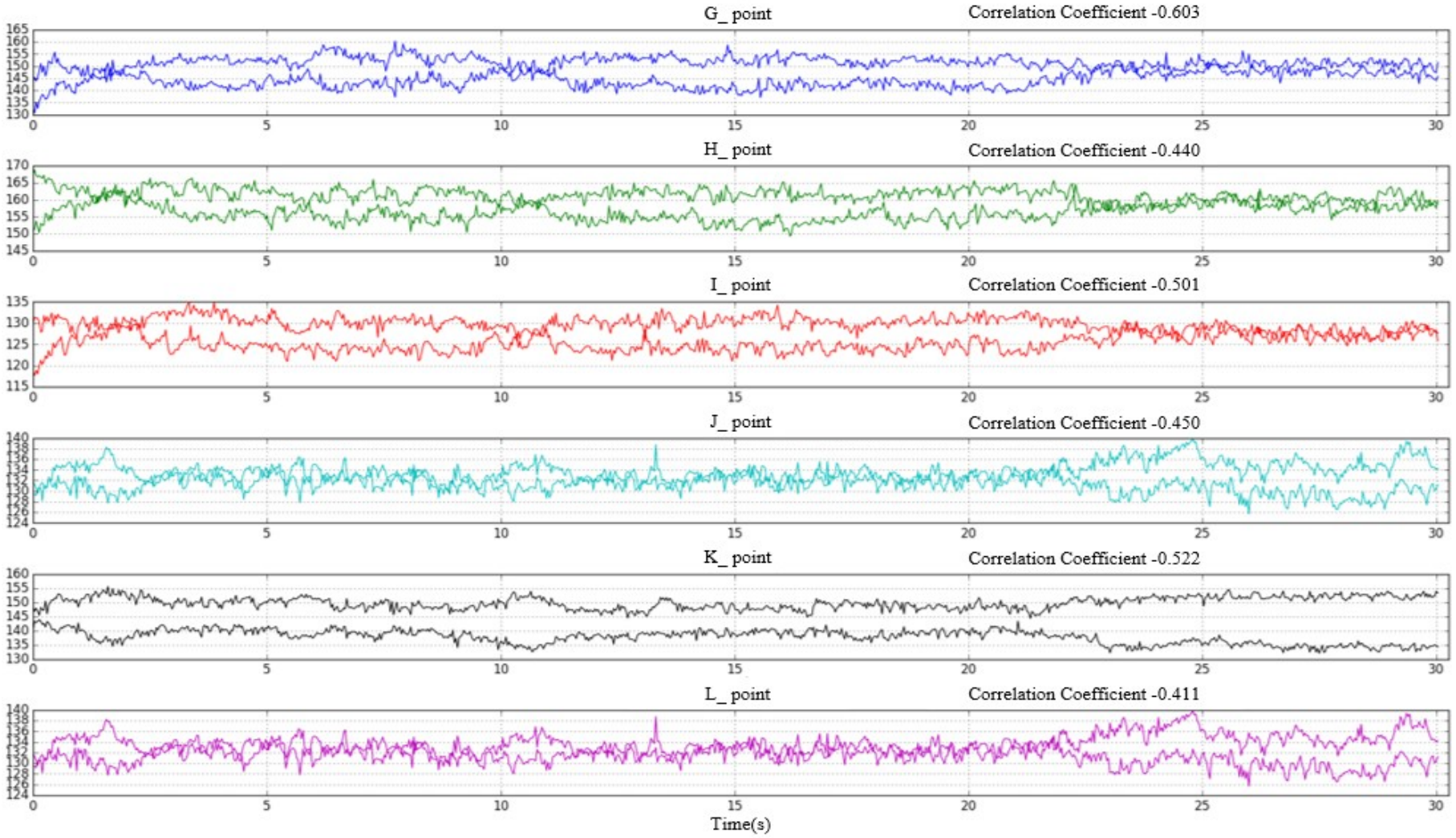
G_ point
Correlation Coefficient -0.603
H_ point
Correlation Coefficient -0.440
I_ point
Correlation Coefficient -0.501
J_ point
Correlation Coefficient -0.450
K_ point
Correlation Coefficient -0.522
L_ point
Correlation Coefficient -0.411
Time(s)

Figure6.7 Time series optical intensity of two regions composed of negatively correlated. These data are spatially different blinking points.

6.3 Conclusion and Discussion

As a result of statistical analysis, it was found that the blinking point is composed of two regions composed of negative correlations. Negative correlation means that as the optical intensity of one increase, the optical intensity of the other decreases. I also found that these two areas are related to the other two areas of the surrounding blinking points and behave as if the blinking intensities were synchronized. However, there were some blinks that behaved in the opposite way when viewed on a long-time scale.

Since the two regions can show a relatively high negative correlation, the number of carriers reaching one blinking point is considered constant, and many carriers are involved in recombination in one region. On the other hand, the number of carriers involved in recoupling may be small in other regions. This means that the QCSE wavefunction overlap increases in one region and decreases in the other. As mentioned in Chapter 2, QCSE is due to the piezo electric field. In addition, since the behavior of the other two blinking regions existing in the surroundings and the behavior of the two regions are synchronized, the application of the piezo electric field is synchronized in the portion where the indium corresponding to the blinking portion is localized. On the contrary, regarding blinking that behaves in the opposite

direction without synchronization, it is considered that the application of the piezo electric field also behaves in the opposite direction. As a future prospect, it is necessary to directly show by experiment whether the magnitude of the piezoelectric field is constantly changing in the blinking part and whether the application of the piezoelectric field is synchronized in the blinking part.

7 The Electronic Properties of Chlorine in GaN (External Collaboration)

Although the main focus of my research is the blinking phenomena, I also elucidated the effects of internal impurities in GaN using ab initio calculations and I published a paper.[21] This work was done in collaboration with Dr. Giovanni Alfieri, who works at ABB Power Grid Research in Switzerland. It is well known that internal impurities can significantly alter the overall functionality of a device, and the presence of this defect cannot be ignored in the development of GaN optoelectronics. For example, it has been reported that nitrogen vacancies in GaN can prevent the formation of p-type GaN. Carbon unintentionally trapped in GaN has also been studied. Carbon is easily replaced by nitrogen in GaN and is known to cause yellow luminescence. Thus, the presence of point defects has been reported to have a negative effect on devices.

We focused on chlorine, which is a chlorine-based reactive ion etching process for the fabrication of GaN semiconductor devices. In this process, chlorine can be unintentionally mixed into GaN. Chlorine-based etching has been reported to reduce the carrier concentration in p-type GaN by two orders of magnitude; in n-type GaN, the ohmic contact resistivity is reported to be reduced or even increased. Although

the above experimental facts have been presented, the overall interpretation is ambiguous. To answer this question, we calculated the defect formation energy by performing SIESTA-based density functional theory [22] for three structures: one with substituted chlorine, one with both vacancies and substituted chlorine, and one with substituted chlorine and magnesium. By calculating the defect formation energy, it is possible to quantitatively evaluate in which charged state the impurity exists stably in the band gap, and whether it behaves as a donor that emits electrons or as an acceptor that receives electrons.

In using SIESTA, Troullier-Martines norm-conserving pseudopotentials [23] was used to take into account the influence of the core electrons, and the Ceparley-Alder form of the local density approximation (LDA) [24] was used to approximate the exchange correlation potential. The double-ζ plus polarization is used as the basis for the atomic orbitals, and the d-orbitals are treated as valence electrons in the Ga atom. The equilibrium configuration of GaN, which contains a total of 96 atoms, was determined using the conjugate gradient method until the maximum nuclear energy was below 0.025 eV and the stress tensor was 0.5 Gpa. The charge density was projected onto a real space grid with a cutoff of 375 Ry. Each grid constant was 1% larger than the experimental value and the direct band gap was 2eV.

The density functional theory calculations show that the chlorine substitution at the N site behaves as a double donor. In the other two, the impure chlorine also behaves as a donor and is responsible for releasing electrons. This could explain the experimental increase in electron concentration in dry-etched n-type GaN.

8 Bibliography

1. THEMIS editorial department Japan. Blue light-emitting diode (2004)

2. D.S.Arteev *et al* Investigation of Statistical Broading in InGaN Alloys 2018 J. Phys.: Conf. Ser. 1135 012050

3. Christian Feldmeier, Blinking Phenomena in InGaN Quantum Wells, University of Regensburg Master's thesis (2009)

4. Josh Abell and T.D. Moustakas, The role of dislocations as nonradiative recombination centers in InGaN quantum wells, Applied Physics Letters,92,091901 (2008)

5. H.Morkoc, S.Strite, G.B.Gao, M.E.Lin, B.Sverdlov, and M.Burns, Large-band-gap SIC,Ⅲ-Vnitride, and Ⅱ-Ⅵ ZnSe-based semiconductor devise technologies, Journal of Applied Physics, Volume76, Issue3 (1994)

6. Y.Narukawa, Y.kawakami, M.Futano, Sz.Fujita. and Sg.Fujita, Role of self-formed InGaN quantum dots for exciton localization in the purple laser diode emitting at 420 nm, Applied Physics Letters, 70,981 (1997)

7. Y.Narukawa,Y.Kawakami,S.Fujita and S.Nakamura, Recobination dynamics of localized excitons in oo multiple quantum wells, PHYSICAL REVIEW B, 55,R1938 (1997)

8. A.Kaneta,M.Futano,and Y.Kawakami, Nanoscopic recombination processes in InGaN/GaN quantum wells emitting violet,blue,and green spectra, PHYSICAL REVIEW B, 78, 125317 (2008)

9. Ruggero Micheletto, Masayoshi Abiko, Akio Kaneta, Yoichi Kawakami, Yukio Nakamura, and Takashi Mukai, Observation of optical instabilities in the photoluminescence of InGaN single quantum well, Applied Physics Letters, 88,061118 (2006)

10. M-E.pistol, P.Castrillo, D.Hessman,J.A.Prieto, and L.Samuelson, Random telegraph noise in photoluminescence from individual self-assembled quantum dots, Physical Review B, VOLUME59,NUMBER16 (1998)

11. D.bertram, M.C.Hanna, and A.J.Nozik, Two color blinking of single strain-induced GaAs quantum dots, Applied Physics Letters 74,2666, (1999)

12. J W.Robinson , J H Rice, Kwan H Lee, Jong H. Na, and R A.Taylor D G.Hasko R A.Oliver, M J.Kappers and C J.Humphreys, G.Andrew D.Briggs,

Quantum-confined Stark effect in a single InGaN quantum dot under a lateral electric field, Applied Physics Letters, 86,213103 (2005)

13. S H.Park and S L.Chuang, Crystal-orientation effects on the piezoelectric field and electronic properties of strained wurtzite semiconductors, Physical Review B, VOLUME59,NUMBER7 (1999)

14. K.Oikawa, Study of optical blinking phenomena on nitride semiconductors, Yokohama City University Graduate School of nanoscience Master thesis (2011)

15. R.J.Cook, and H.J.Kimbie, Possibility of Direct Observation of Quantum Jumps, PHYSICAL REVIEW LETTERS, VOLUME54, NUMBER 10

16. M.Nirmal, B.O.Dabbousi, M.G.Bawendi, J.J.Macklin, J.K.Trautman, T.D.Harris and L.E.Brus, Fluorescence intermittency in single cadnium selenide nanocrystals, Nature 383,802-804 (1996)

17. T.Tsutsumi, The influence of surface conditions in InGaN quantum well photoluminescence dynamics, Yokohama City University Graduate School of nanobioscience Master's thesis (2015)

18. T.Tsutsumi, G.Alfieri, Y.Kawakami, R.Micheletto, The relation between photoluminescence properties and gas pressure with [0001] InGaN single quantum well systems, Applied Surface Science 392, 256-259 (2017)

19. USHIO Specification Sheet, USH-102D, USHIO Super High Pressure UV Lamp (https://www.ushio.co.jp/documents/products/light_source/USH102D_J.pdf)

20. Modified version provided by Olympus Corporation (I received 2020 7/30)

21. Y.Fujii, R.Micheletto, and G.Alfieri, The Electronic Properties of Chlorine in GaN: An Ab Initio Study, Physical Status Solidi B, 2000303 (2020)

22. J.M.Soler, J.D.Gale, A.Garcia, J.Junquera, P.Ordejon, and D.Sanchez-Portal, The SIESTA method for ab initio order-N materials simulation, Journal of Physics, Condens.Matter 14 2745 (2002)

23. N.Troullier and J.L. Martins, Efficient pseudopotentials for plane-wave calculations, Physical Review B, 43,1993 (1991)

24. D.M.Ceparly and B.J.Alder, Ground State of the Electron Gas by a Stochastic Method, Physical Review letters, 45,566 (1980)

9 Acknowledgement

I would like to thank Professor Ruggero Micheletto for his very enthusiastic guidance in conducting this research on myself. He also taught me about programming and helped me to develop skills that I can use in the future as a member of society. I would like to express my deepest gratitude to him.

Professor Yoichi Kawakami of Kyoto University also gave me extensive guidance on knowledge. Thanks to Dr. Kawakami's advice, I was able to conduct meaningful research. I would like to express my deepest gratitude to him.

Dr. Giovanni Alfieri, who belongs to Hitachi Power Grid, Lenzburg, Switzerland, gave me knowledge about first-principles calculations. I asked a lot of questions by e-mail every day, but I received accurate and easy-to-understand answers from him. I would like to express my deepest gratitude to him.

I would also like to thank Mr.K.Sano of Katsumichi Corporation for providing me with useful instruments for measurements. I would like to express our deepest gratitude to him.

I would like to thank Mr. Rei Maekawa and Mr. Kazuki Konno, who graduated from our laboratory last year, for their precise advice mainly on seminar activities.

We had a very meaningful time together outside of research activities, such as discussions over drinks. I would like to express my deepest gratitude to them.

I would like to thank Makoto Ono and Akira Hirai, who are my classmates in the laboratory, we were able to work hard and polish each other's research for two years. Although they sometimes gave me harsh advice, it was because of them that I was able to conduct good research. I am deeply grateful to them.

I have fond memories of not only discussing my research with Yoshinori Tsuchiya and Kenya Tsukada, who are one year behind me, but also discussing about my future and job hunting activities. It was a great opportunity for me to learn something that I did not know before. I would like to express my deepest gratitude to them.

I was able to discuss with Masaya Tsukida and Yuya Okajima, who are two years behind me, from morning till night in the laboratory. We were able to discuss not only our own research, but also how each other's research could be useful in the future. They taught me a lot about statistics and increased my curiosity about statistics. I would like to express my deepest gratitude to them.

For a short time, I was able to have an intense discussion with Shunra Yoshida, who is three years my junior, about the blinking phenomena. I was amazed at the amount of knowledge he had. I would like to express my deepest gratitude to him.

I would like to thank my family for supporting me for the past 24 years in good health.

10 Conferences and Publications

[Conference Oral Presentation]

1. International Workshop on Nitride Semiconductors 2020, August 23-28, 2020 in Berlin, Germany. (Oral session)

Title: The effect of absorbed liquids on the optical blinking of InGaN/GaN quantum Wells

2. Nano-Optics Research Group 27th Research Discussion Meeting (Japan). January 22 2021 (Oral session held online)

Title: Study on unstable blinking phenomenon on InGaN/GaN single quantum well

ナノオプティクス研究グループ第27回研究討論会 オンライン開催　2021年　1月22日

発表題目　InGaN/GaN 単一量子井戸型構造上の不安定点滅現象に関する研究

[Publication]

Y.Fujii, R.Micheletto, and G.Alfieri, The Electronic Properties of Chlorine in GaN:

An Ab Initio Study, Physical Status Solidi B, 2000303 (2020)

11 Summary of the research (Japanese)

【日本語要旨】

発光デバイスに使われるInGaN/GaN単一量子井戸型構造上(InGaN/GaN SQW)に励起波長365nmの紫外線を照射すると、表面に不安定な点滅を繰り返す無数の輝点が発生する。これはInGaN以外の量子ドットでも観測されるが、原因不明な現象の一つでありメカニズムの解明が求められている。そこで、本研究ではこの不安定点滅現象の物理学的なメカニズムを解明することを目的とし、点滅現象の温度依存性、液体の付着による点滅現象の変化、さらに、統計的な分析を行うことで点滅点の相関関係などを調査した。

第1章ではInGaN窒化物半導体の開発の歴史と基礎的な物性についてまとめた

第2章ではミケレット･ルジェロらによって発見されたInGaN/GaN SQW上の点滅現象についての具体的な説明、点滅現象の要因とされている物理学的モデルや過去の先行研究事例についてまとめた。

第3章では実験に利用したInGaN/GaN SQWの内部構造、本研究で利用したオリンパス社製の選択励起蛍光顕微鏡のメカニズム、得られたビデオデータの処理方法についてまとめた。

第4章にて点滅現象の温度依存性について、発光波長が460nmと510nmのInGaN/GaN SQWを利用することで検討を行った。両サンプルに共通して、相対的に低い温度環境で光励起を行うと点滅が発生しやすい結果が得られた。また、温度上昇により点滅の激しさが和らぎ、点滅点も消滅していく傾向が見られ、発光波長が460nmのInGaN/GaN SQWでは最高温度の373Kにて、90%以上の点滅が消滅した。510nmの場合も同様に温度上昇によって点滅の激しさは和らいでいくが、最高温度の373Kでも点滅し続ける輝点が存在している結果となった。温度上昇による熱膨張が数多くの欠陥を生成し、キャリアが欠陥にトラップされやすくなったが故に非輻射再結合を行うようになった結果、点滅の激しさが和らいだと私は考えている。他の要因として電子移動度の低下などが挙げられるが、温度上昇によりあらゆる物理量が変化するため、明確な原因については本研究で突き止めることができなかった。

第5章では液体を付着させた状態で光励起を行い、点滅の挙動を観察した。利用した液体は水とエタノールであり、何も付着させていない状態との比較を行った。試料は、第4章と同様に発光中心波長が460nmと510nmの2種類を利用している。こ

の結果、液体の付着が点滅現象を誘発していることが両者共通して明らかとなった水を付着させた場合、輝点が増え、点滅の激しさが若干増すが、エタノールの場合、点滅が非常に激しくなる現象が顕著に見られた。液体の付着がInGaN/GaN SQW内部の電子状態を変え、点滅を引き起こしやすい環境を作り出していることが示唆される。仮説としては、価電子帯近傍の状態密度が大きくなり、励起に必要な電子の席が増えた。または、点滅現象が量子閉じ込めシュタルク効果により発生しているのであれば、点滅箇所におけるピエゾ電界の印加の大きさが高速で増減を繰り返していると考えられる。

第6章では統計的分析により、点滅は負の相関である2つの領域で構成されていることが明らかになった。負の相関とは、2つの領域のうち片方の光学強度が上昇すれば、もう片方が下降していく現象が1フレーム毎（約0.03秒）に発生していることを意味する。また、1つの点滅点だけでなく、周囲に存在している他の点滅とも相関性が見られ、点滅内の2つの領域の光学強度が同期しているような振る舞いをしていることが分かった。すなわち、約0.03秒毎に光学強度が相関性を示すだけでなく、長い時間スケールで考えても、光学強度が相関性を示していることになる。仮に点滅現象が量子閉じ込めシュタルク効果により引き起こされているならば、点滅箇所に印加されるピエゾ電界の大きさも時系列的に同期していると考えられ、再結合率も同期すると考えることができる。点滅が負の相関を示すことについては、片方の領域ではピエゾ電界の大きさが大きくなりキャリアの再結合率が下がっていくが、もう片方では対照的な現象が発生しているからと考える。

第7章ではスイスの日立パワーグリップ社に所属する、ジョバンニ・アルフィエリ博士との共同研究について簡単にまとめた。窒化ガリウム（GaN）の製造プロセスの1つである反応性イオンエッチングにおいて、塩素が混入されてしまうことが示唆されており、塩素が混入された場合のGaNの物性について明らかにされていない。そこで第一原理計算ソフトの一つであるSIESTAを利用した密度汎関数法を実行し、欠陥生成エネルギーを算出することで不純物塩素が含まれたGaNの電子物性について定量的に評価した。結果としてGaN内部の塩素は電子を放出することで安定な構造をとるドナーとしてGaN内部で振る舞うことが明らかになった。

続く第8章は参考文献、第9章は謝辞から構成され、第10章に研究実績をまとめた。